AD ________________

GRANT NUMBER DAMD17-96-1-6050

TITLE: Genes Determining Taxol Sensitivity

PRINCIPAL INVESTIGATOR: Hongming Zhu

CONTRACTING ORGANIZATION: University of Illinois
Chicago, Illinois 60612-7205

REPORT DATE: September 1999

TYPE OF REPORT: Final

PREPARED FOR:
U.S. Army Medical Research and Materiel Command
Fort Detrick, Frederick, Maryland 21702-5012

DISTRIBUTION STATEMENT: Approved for public release;
distribution unlimited

REPORT DOCUMENTATION PAGE

Form Approved
OMB No. 0704-0188

1. AGENCY USE ONLY *(Leave blank)*	2. REPORT DATE	3. REPORT TYPE AND DATES COVERED
	September 1999	Final (1 Aug 96 - 1 Aug 99)

4. TITLE AND SUBTITLE Genes Determining Taxol Sensitivity

5. FUNDING NUMBERS DAMD17-96-1-6050

6. AUTHOR(S)

Hongming Zhu

7. PERFORMING ORGANIZATION NAME(S) AND ADDRESS(ES)

University of Illinois
Chicago, Illinois 60612-7205

8. PERFORMING ORGANIZATION REPORT NUMBER

9. SPONSORING/MONITORING AGENCY NAME(S) AND ADDRESS(ES)

U.S. Army Medical Research and Materiel Command
Fort Detrick, Frederick, Maryland 21702-5012

10. SPONSORING/MONITORING AGENCY REPORT NUMBER

11. SUPPLEMENTARY NOTES

12a. DISTRIBUTION / AVAILABILITY STATEMENT

Approved for public release; distribution unlimited

12b. DISTRIBUTION CODE

13. ABSTRACT *(Maximum 200*

To identify genes determining tumor cell sensitivity to taxol, we have carried out expression selection of genetic suppressor elements (GSEs) that would render cells resistant to taxol. Human cells were transduced with a retroviral library of normalized cDNA fragments, and several putative GSEs were isolated by consecutive rounds of taxol selection, recovery of integrated retroviruses and re-transduction of recipient cells. Based on the mitochondrial origin of one of the putative GSEs, we have developed cell lines lacking in mitochondrial DNA and found that such lines are cross-resistant to several drugs but not to taxol. The tested candidate GSEs conferred taxol resistance in some but not all experiments; this result most probably reflects a requirement for co-transduction of cells with some additional GSEs, as found in another GSE selection project. To improve future selection and testing of GSE combinations, we have developed novel retroviral vectors carrying green fluorescent protein as a marker gene, as well as methods for using such vectors and for efficient recovery of integrated retroviruses. Finally, we found that treatment of breast carcinoma cells with different anticancer agents induces a senescence-like phenotype associated with permanent growth arrest; augmentation of this response may be beneficial for breast cancer therapy.

14. SUBJECT TERMS Breast Cancer , taxol, genetic suppressor elements, retroviral vectors, green fluorescent protein, cell senescence

15. NUMBER OF PAGES 47

16. PRICE CODE

17. SECURITY CLASSIFICATION OF REPORT	18. SECURITY CLASSIFICATION OF THIS PAGE	19. SECURITY CLASSIFICATION OF ABSTRACT	20. LIMITATION OF ABSTRACT
Unclassified	Unclassified	Unclassified	Unlimited

NSN 7540-01-280-5500

Standard Form 298 (Rev. 2-89)
Prescribed by ANSI Std. Z39-18
298-102

FOREWORD

Opinions, interpretations, conclusions and recommendations are those of the author and are not necessarily endorsed by the U.S. Army.

____ Where copyrighted material is quoted, permission has been obtained to use such material.

____ Where material from documents designated for limited distribution is quoted, permission has been obtained to use the material.

H.Z. Citations of commercial organizations and trade names in this report do not constitute an official Department of Army endorsement or approval of the products or services of these organizations.

____ In conducting research using animals, the investigator(s) adhered to the "Guide for the Care and Use of Laboratory Animals," prepared by the Committee on Care and use of Laboratory Animals of the Institute of Laboratory Resources, national Research Council (NIH Publication No. 86-23, Revised 1985).

____ For the protection of human subjects, the investigator(s) adhered to policies of applicable Federal Law 45 CFR 46.

H.Z. In conducting research utilizing recombinant DNA technology, the investigator(s) adhered to current guidelines promulgated by the National Institutes of Health.

H.Z. In the conduct of research utilizing recombinant DNA, the investigator(s) adhered to the NIH Guidelines for Research Involving Recombinant DNA Molecules.

____ In the conduct of research involving hazardous organisms, the investigator(s) adhered to the CDC-NIH Guide for Biosafety in Microbiological and Biomedical Laboratories.

Hongming Zhu 8/25/99
PI - Signature Date

TABLE OF CONTENTS

(5) INTRODUCTION

Chemotherapeutic treatment, based on antiestrogens (such as tamoxifen) or cytotoxic chemotherapeutic drugs (doxorubicin, cyclophosphamide, methotrexate, 5-fluorouracyl) has shown limited efficacy in the treatment of breast cancer (Harris et al., 1993). The major new drug to enter the chemotherapeutic armamentarium for this malignancy in the past two decades is taxol, an alkaloid extracted from the bark of *Taxus brevifolia.* In different clinical trials, taxol-induced response rate in breast cancer varied from 20 to over 60% depending on regimen, dose and prior treatment (Arbuck et al., 1994). Objective response was found even in metastatic cancers resistant to doxorubicin or other means of extensive therapy (Arbuck et al., 1994; Buzdar et al., 1995; Seidman et al., 1993). However, a substantial number of tumors demonstrated only a partial response or no response at all. Understanding the molecular determinants of taxol sensitivity or resistance in breast carcinoma cells is likely to result in the development of chemotherapeutic regimens aimed at avoiding or reversing clinical resistance to taxol. The aim of the present study has been to identify the genes that determine the sensitivity of human cells to taxol. Our approach to the identification of chemotherapeutic sensitivity genes was based on the isolation of genetic suppressor elements (GSEs), that would be derived from such genes and that would induce cellular resistance to taxol. GSEs are short cDNA fragments that counteract the genes from which they are derived by encoding inhibitory peptides or antisense RNAs (Holzmayer et al., 1992). Our laboratory has previously developed the methodology for GSE selection from retroviral libraries carrying short random fragments of normalized cDNA from mammalian cells and identified several GSEs conferring resistance to anticancer drugs (Gudkov et al., 1994; Roninson et al., 1995). The same strategy has been applied in the present project to isolate GSEs that would render human cells resistant to taxol and to identify genes giving rise to such GSEs.

(6) BODY

1. Introduction of a normalized retroviral cDNA library into HT1080 cells and taxol selection (E.S. Kandel) (Task 1-4).

A library of randomly oriented normalized short cDNA fragments of human HeLa cells has been constructed in our laboratory (Levenson et al., 1999) using retroviral vector pLNCX, which carries *neo* (G418 resistance) gene as the selectable marker (Miller and Rosman, 1989). For the target cell line, we have engineered HT1080 human fibrosarcoma cells to express the cDNA for murine ecotropic receptor (Albritton et al., 1989). This modification enabled us to use very efficient transduction with high titer ecotropic retroviruses that are free of helper virus and not infectious to humans. The ecotropic-receptor transduced cell line, HT1080/E14, appears to be a suitable model for drug response in human cells, as it is sensitive to all chemotherapeutic compounds tested, including taxol. The library has been introduced into HT1080/E14 cells, and the infected population (~$4x10^6$ independent infectants) was subjected to two rounds of taxol treatment. In the course of this selection, we developed a new method for provirus rescue based on long-range PCR amplification of the entire integrated proviruses (Schott et al., 1997; see the attached reprint), and used this technique to transfer the reduced complexity provirus mixtures into fresh populations of HT1080/E14 cells (secondary infectants). After another round of provirus transfer and taxol selection, PCR analysis revealed retention of 1-8 individual inserts in each experimental population. Noticeably higher survival of taxol was observed in experimental cells relative to vector-infected control, suggesting that secondary and tertiary infected populations may in fact be enriched for cells containing active GSEs.

2. Sequencing and initial testing of putative GSEs enriched by taxol selection (E.S. Kandel) (Tasks 5-7, 9).

We have isolated a number of individual cDNA fragments enriched in separate populations of secondary and tertiary infectants. Putative GSEs were sequenced and compared to the known sequences deposited in GenBank. Three candidate GSEs were chosen for further analysis, based on the relative resistance of the populations from which they were isolated and their representation in such populations. The sequences of these GSEs are presented in Fig 1a,b,c. One of the putative GSEs, designated 2c1, corresponds to a fragment of both translation elongation factor E1α and proto-oncogene *PTI* (Shen et al., 1995). The second element, 302, originates from an unknown gene. The third sequence, 2a1, was derived from human mitochondrial gene *COXIII*, which encodes a subunit of cytochrome *c* oxidase. A GSE that closely overlaps (but is not identical) with 2a1 was independently isolated in our laboratory through the selection for resistance to a replication inhibitor aphidicolin (Levenson et al., 1999), and therefore this clone attracted our particular attention. These putative GSEs were cloned into LNCX and introduced into naive HT1080/E14 cells via retroviral transduction. Initial testing was carried out with 100%-infected populations that were obtained after G418 selection. Some experimental populations appeared to have increased resistance to taxol relative to vector-transduced cells, based on cell survival assays, but this result could not be consistently reproduced for any of the candidate GSEs. We hypothesized therefore that these GSEs may have a weak effect that may not be readily detectable by cell survival assays. Since, however, these GSEs were enriched in the original taxol selection, we could expect that a test that measures changes in the percentages of transduced cells carrying such GSEs may indicate that taxol selects for such GSEs. In order to measure such changes, and also to avoid G418 selection that other studies in our lab found to be detrimental for gene expression from LNCX-type vectors (Schott et al., 1996), we set out to develop and test retroviral vectors that would carry the Green Fluorescent Protein (GFP) rather than *neo* as the selectable marker.

3. Development of a series of GFP-containing retroviral vectors for GSE selection and testing (E.S. Kandel; see attached reprint of Kandel et al., 1997).

GFP of *Aequorea victoria* is used as a vital fluorescent tag for the detection and isolation of genetically modified cells. We have tested several modified variants of GFP as marker genes in retroviral vectors containing different backbones and promoter combinations. Constructs allowing for reliable detection of GFP fluorescence and the expression of a cotransduced gene from a strong promoter were identified. Cells harboring such constructs were shown to be detectable by flow cytometry, fluorescence microscopy and multi-well fluorescence reading. GFP expression in transduced cells was found to be stable both *in vitro* and *in vivo*. Most importantly for the present project, we have found (using p53 tumor suppressor as a prototype gene affecting the cell growth) that long-term dynamics of GFP-positive fractions in a mixed population can be used to monitor the biological effects of a cotransduced gene. We have also shown that selection of cells with the highest GFP fluorescence enriches for multiply infected cells, an important result for the use of GFP vectors to study the effects of GSE combinations (see the next section). Furthermore, the use of different GFP variants allows one to monitor simultaneously two cell populations transduced with vectors carrying GFPs that differ in their fluorescence intensity or spectral properties and to identify doubly transduced cells. In addition, we have shown that transcription of an inducible promoter positioned in the opposite orientation to GFP can be monitored by the inhibition of GFP fluorescence. Our study demonstrated that GFP provides a useful marker for gene transfer by retroviral vectors, extending the range of applications for retroviral transduction (Kandel et al., 1997).

Figure 1. Sequences of putative GSEs enriched by taxol selection.

2c1 (a segment of cDNA for elongation factor E1α and proto-oncogene *PTI)*

ATGGATGGATGGAGAATGGGCAGACCCGANAGCATGCCCTTCTGGCTTACA
CACTGGGTGTGAAACAACTAATTGTCGGTGTTAACAAAATGGATTCCACTGA
GCCACCCTACAGCCAGAAGAGATATGAGGAAATTGTTAAGGAAGTCNGCAC
TTACATTAAGAAAATTGGCTACNACCCCGCCATCCATCCATCGAT

302 (anonymous sequence, a segment of clone hRPK.651_L_9 from chromosome 17)

AGAACGACCACCGGGACCGATCCAGAATCCGCGGCCCCAAGCTTGTTAAC
ATCCATGGATGGATGGGCAGAGCAGGCGGGGTCCCAAGTCAGCAGTCGAG
GTCCTGCTAATGCTCAGAACACAGGACCAACAGACAGGTCTGTACTGCCCA
CCCTCAGTTCTTTACAGTGAAGAGAAGCGCTGGACTTCAGAGACACTTAGG
AC

2a1 (a segment of mitochondrial *COXIII* gene)

GATTGGTATATGGTTAGTGTGTTGGTTAGTAGGCCTAGTATGAGGAGCGTTA
TGGAGTGGAAGTGAAATCACATGGCTAGGCCGGAGTCATTAGGAGGGCTG
AGAGGCCCTGTTAGGTCACGGGCC

Treatment	Vector-transduced	GSE2a1-transduced	GSE2c1-transduced	GSE302-transduced
No drug	15.0%	14.4%	19.1%	16.2%
Regimen 1	14.8%	15.3%	17.8%	15.9%
Regimen 2	15.0%	15.7%	20.7%	14.7%

Figure 2. Fraction of GFP-positive cells in GSE-transduced populations upon taxol treatment.

HT1080 cells were transduced with LmECX vector or with the same vector harboring GSE2a1, GSE2c1 or GSE302 inserts. $5x10^5$ cells of each population were treated with taxol. Regimen 1 included a 2-day exposure to 3ng/ml of drug. Regimen 2 included an additional replating of the surviving cells (after a 3-day recovery period) followed by a 2-day exposure to 5 ng/ml of taxol. Fraction of GFP-positive cells was measured after completion of cell dying and resumption of growth by the surviving population. Results were compared to the values in respective untreated controls. Flow cytometry was performed on Becton Dickinson FACSort instrument and the data was analyzed using CellQuest software. Only viable cells of normal morphology (as judged by propidium iodide exclusion criterion, forward and side scatter readings) were included in the analysis.

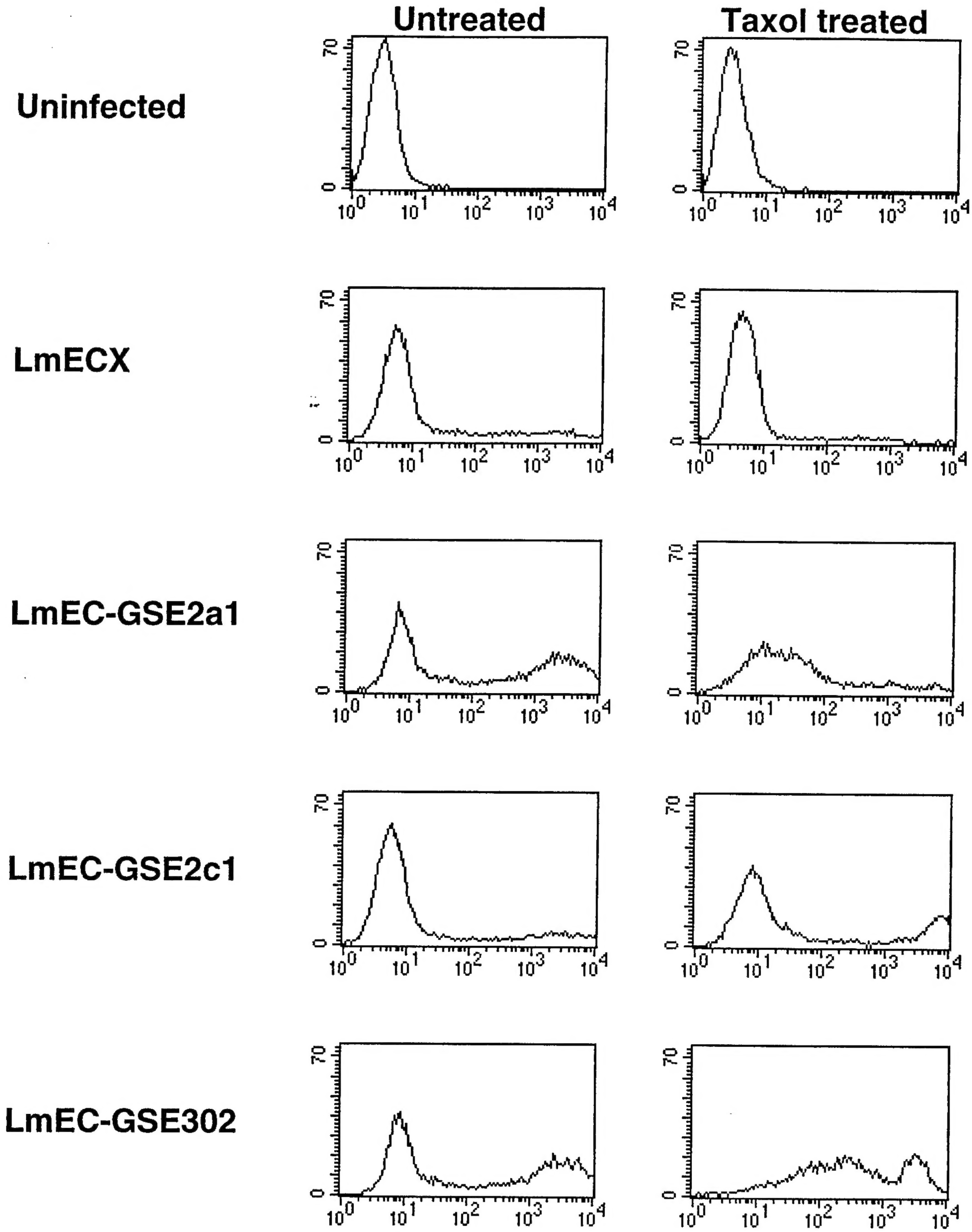

Figure 3. Effect of high-dose taxol treatment on the composition of transduced populations.

HT1080 cells transduced with LmECX vector or the same vector harboring GSE2a1 (LmEC-GSE2a1), GSE2c1 (LmGC-GSE2c1) or GSE302 (LmEC-GSE302) were treated with taxol (10 ng/ml) for 2 days and analyzed as described in Figure 2. Data is plotted as a number of cells versus fluorescence.

4. Testing taxol-selected candidate GSEs in a GFP-containing vector (E.S. Kandel) (Tasks 6-7).

We have introduced the 2c1, 302 and 2a1 sequences, that were enriched by taxol selection, into a GFP-containing vector LmECX (Kandel et al., 1997), and transduced these constructs, as well as insert-free LmECX vector, into HT1080/E14 cells. To test if the candidate GSEs would be enriched after taxol selection, we treated the newly transduced cell populations with taxol and monitored changes in the frequency of GFP-positive cells by FACS. In most experiments, however, we failed to observe any significant changes in the fraction of GFP-positive cells before and after treatment with taxol (Fig. 2). The only situation when a transduced population appeared highly enriched, were several experiments conducted at a very high dose of paclitaxel, when $<10^2$ taxol-surviving colonies arose from $5x10^5$ treated cells (Fig. 3).

These negative results are best explained in light of a concurrent study in our laboratory (Levenson et al., 1999), where a similar selection was carried out for GSEs conferring resistance to aphidicolin. In that study, reproducible resistance was achieved only when cells were coinfected with four GSEs derived from different genes, including one that was derived from *COXIII* and is nearly identical to our 2a1 clone. As in the present study, transduction with individual GSEs produced weakly positive results that were not consistently reproducible. In contrast, the combination of the four GSEs reproducibly rendered cells resistant to aphidicolin, doxorubicin and hydroxyurea, but not to taxol. Interestingly, the resistance conferred by the GSE combination appears to be associated with decreased induction of the senescence-like response in drug-treated cells (see below) (Levenson et al., 1999). These results suggest that the candidate GSEs isolated after taxol selection, especially 2a1, may be components of a combination that produces resistance to taxol, but other required members of this combination have not been isolated in our selection. Future GSE selections should be carried out in a way that would maximize the isolation of all members of each active combination. The success of the aphidicolin study was enabled by comprehensive analysis of retroviral inserts integrated in individual drug-selected cellular clones, an approach that was not used in the present project. Future GSE selections should benefit, however, from the vectors and methods developed in the present study, including GFP-containing retroviral vectors that allow one to isolate cells coinfected with multiple viruses (on the basis of high GFP fluorescence) (Kandel et al., 1997) and the very efficient recovery technique based on long-range PCR (Schott et al., 1997).

5. Generation of a subline of HT1080 cells lacking mitochondrial DNA and analysis of its drug response (H. Zhu).

Since *COXIII*-derived GSEs were enriched in two independent GSE selection projects, we have taken a closer look at the significance of mitochondrial functions and the mitochondrial genome in drug response. For this purpose, we have developed HT1080/E14 derivatives that are devoid of mitochondrial DNA (designated ρ-). These cells were isolated after 35 days of treatment with 50 ng/ml ethidium bromide in the presence of 110 μg/ml sodium piruvate and 100 μg/ml uridine. Southern hybridization (not shown) and PCR (Fig. 4) confirmed the absence of mitochondrial DNA in at least two of the selected clones (1ρ- and 16ρ-). Drug resistance of these ρ- clones, relative to the parental cell line, was analyzed by treating cells with different drug doses for the period of time corresponding to two cell generations of each cell line, followed by 3-4 days of growth in drug-free media and determining relative cell numbers by methylene blue staining (Fig. 5). These assays showed increased resistance of ρ- cells to several replication-inhibiting drugs, including cytarabine, aphidicolin, etoposide and doxorubicin, but not to taxol or vinblastine. We are characterizing the mechanism of this effect; preliminary results suggest that ρ- cells show a decreased induction of the senescent phenotype (see below) after treatment with some of the drugs.

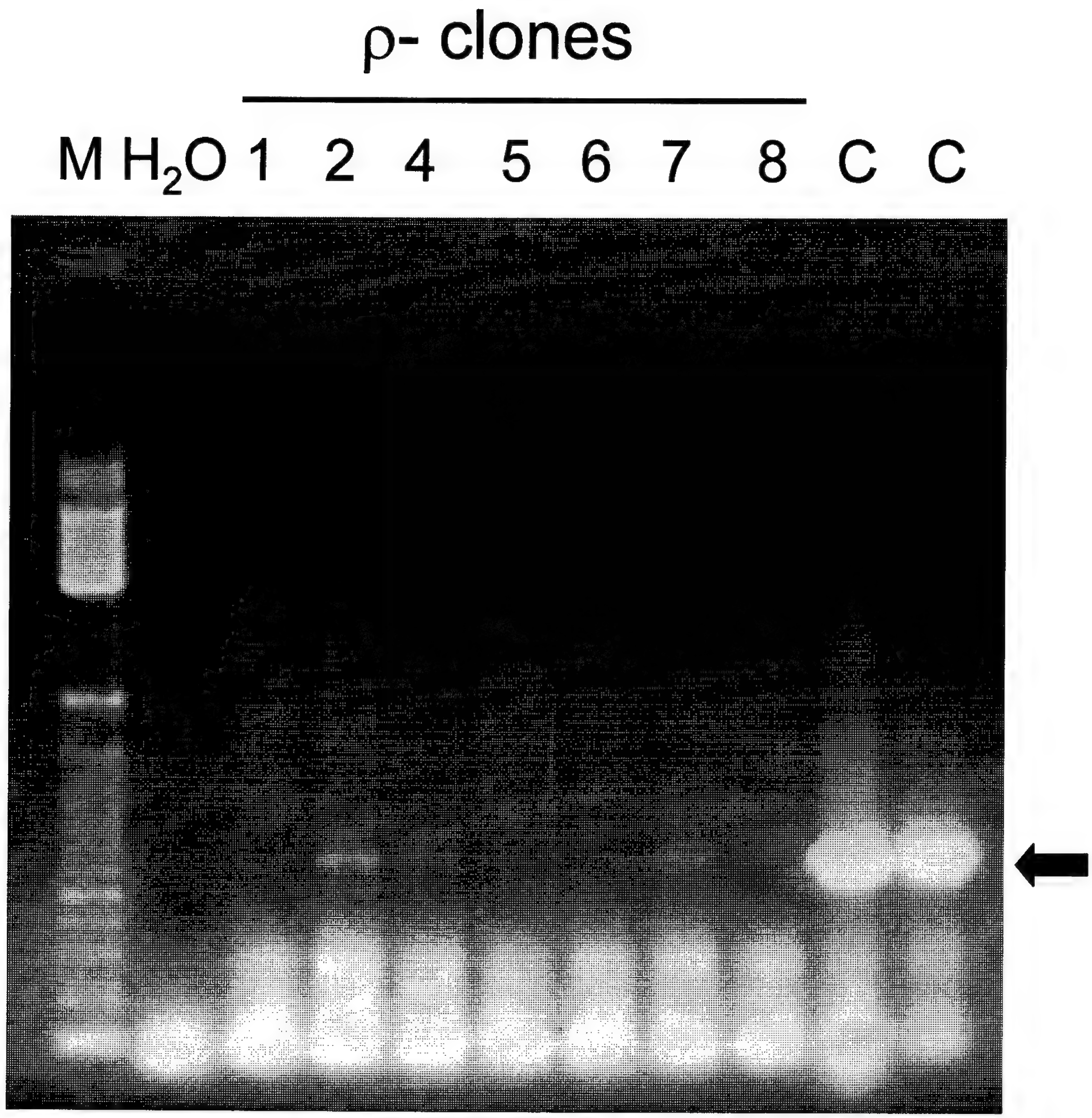

Figure 4. Lack of mitochondrial DNA in ρ- clones isolated from HT1080 cell line.

A representative PCR assay for the amplification of a segment of the mitochondrial COXIII gene in two control populations of HT1080 cells (C) and in seven ρ- clones. The *COXIII*-specific PCR product is marked with an arrow. Note lack of such product in the ρ-clone 1.

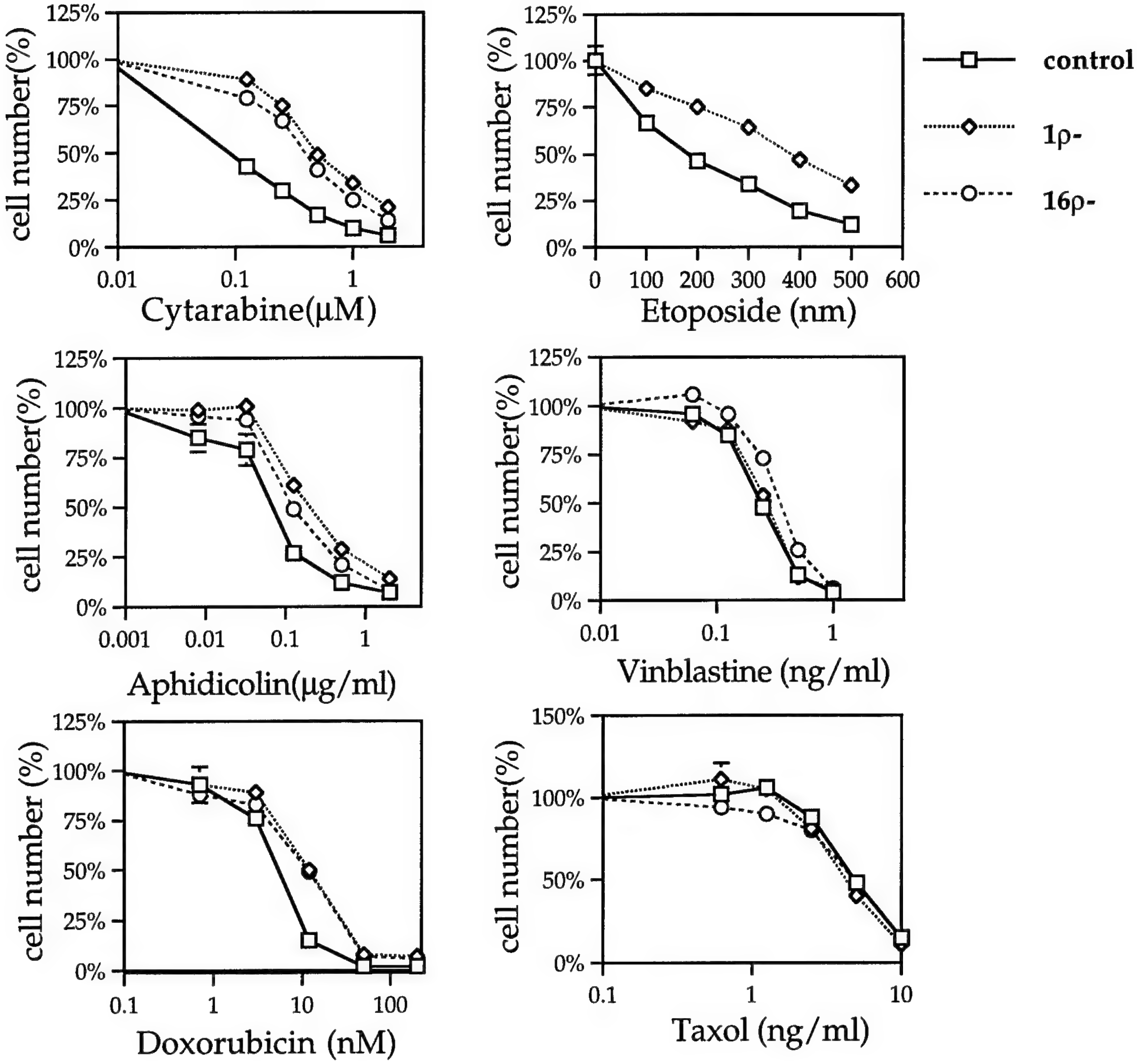

Figure 5. Analysis of drug resistance in 1ρ– and 16ρ– cell lines, lacking mitochondrial DNA, relative to control HT1080 cells.
See text for the description of the assay.

6. Characterization of the senescent-like phenotype induced in breast carcinoma cells by anticancer agents (H. Zhu and E.S. Kandel; see attached reprint by Chang et al., 1999).

Studies that were initially carried out by other investigators in our laboratory revealed that treatment of HT1080 cells with different anticancer agents induces phenotypic markers of cell senescence, including enlarged and flattened morphology, increased granularity, and expression of senescence-associated β-galactosidase activity (SA-β-gal). These markers distinguished those cells that became terminally growth-arrested within a small number of cell divisions from the cells that recovered and resumed proliferation. We have examined the appearance of this phenotype after drug treatment in other tumor-derived cell lines, including breast carcinoma lines MCF-7 and MDA-MB-231. Treatment with a moderate dose of doxorubicin induced the senescent-like phenotype in MCF-7 cells (wild-type for p53) but not in MDA-MB-231 (mutated for p53). Other studies from our lab confirmed the role of p53 in this response (Chang et al., 1999a). We have also tested if treatment of breast carcinoma cells with differentiation-inducing retinoids would induce the senescent phenotype. We have found that treatment of MCF-7 cells with all-trans retinoic acid indeed efficiently induced the markers of senescence; the appearance of these markers correlated with permanent growth arrest. The induction of senescence was also observed in xenografts of MCF10AneoT cells treated in vivo with another retinoid, 4-hydroxyphenyl retinamide (frozen xenograft samples were obtained from Dr. K. Christov of the Department of Surgical Oncology). Thus, induction of a senescence-like program of terminal proliferation arrest may be an important determinant and a potential target for augmentation in breast cancer therapy (Chang et al., 1999).

(7) KEY RESEARCH ACCOMPLISHMENTS

- A new procedure for the recovery of integrated retroviruses has been developed
- A series of new retroviral vectors carrying the Green Fluorescent Protein as a marker, and novel applications for such vectors have been developed
- Derivatives of HT1080 cells lacking mitochondrial DNA have been developed and their resistance to different chemotherapeutic drugs has been characterized
- Induction of senescence-like terminal proliferation arrest has been identified as an important component of cellular response to anticancer agents in breast carcinoma cells

(8) REPORTABLE OUTCOMES

Articles:

Schott, B., Kandel, E.S., and Roninson, I.B. (1997). Efficient recovery and regeneration of integrated retroviruses. *Nucleic Acids Res.* 25, 2940-2942.

Kandel, E.S., Chang, B.D., Schott, B., Shtil, A.A., Gudkov, A.V., and Roninson, I.B. (1997). Applications of Green Fluorescent Protein as a Marker of Retroviral Vectors. *Somatic Cell Mol. Genet.* 23, 325-340.

Chang, B.D., Broude, E.V., Dokmanovic, M., Zhu, H., Ruth, A., Xuan, Y., Kandel, E.S., Lausch, E., Christov, K. and Roninson, I.B. (1999). A senescence-like phenotype distinguishes tumor cells that undergo terminal proliferation arrest after exposure to anticancer agents. Cancer Res. 59, 3761-3767.

Meeting Abstracts:

B. Schott, E. S. Kandel, I. B. Roninson. Efficient recovery and regeneration of integrated retroviruses. Cold Spring Harbor Laboratory Meeting "Retroviruses", Cold Spring Harbor, NY (1997)

E. S. Kandel, B. Schott, B.-D. Chang, A. V. Gudkov, I. B. Roninson. Novel retroviral vectors expressing red-shifted variants of green fluorescent protein. Cold Spring Harbor Laboratory Meeting "Retroviruses", Cold Spring Harbor, NY (1997)

E.Kandel, B.Chang, B.Schott, A.Shtil, V.Levenson, A.Gudkov, I. Roninson. GFP in retroviral vectors: applications and lessons. "International Symposium on Green Fluorescent Protein", New Brunswik, NJ (1997).

Levenson, V.V., Lausch, E., Libants, S., Kirschling, D.J., Kandel, E., and Roninson, I.B. A combination of genetic suppressor elements produces resistance to drugs inhibiting DNA replication. Proc. of the 90th Annual Meeting of the American Association for Cancer Research, Abs. #2818.

Chang, B.-d., Broude, E.V., Zhu, H., Xuan, Y., Dokmanovic, M., Ruth, A., Kandel, E.S., Lausch, E., Christov, K., and Roninson, I.B. Low doses of anticancer agents induce a senescence-like phenotype and mitotic death in human tumor cells. Proc. of the 90th Annual Meeting of the American Association for Cancer Research, Abs. #88.

Degrees obtained:

Eugene S. Kandel, supported by this fellowship, has obtained a PhD degree in Molecular Genetics in July of 1998.

Employment of training and experience supported by this award:

Eugene S. Kandel, PhD, currently holds the position of Research Assistant Professor at the University of Illinois at Chicago

(9) CONCLUSIONS

In the present project, we have used taxol selection of cells transduced with a retroviral library carrying normalized cDNA fragments to isolate several candidate GSEs that were enriched by taxol selection. We were unable, however, to obtain reproducible taxol resistance after transduction of cells with these putative GSEs. The likely reason for this failure has been indicated by concurrent studies by other investigators in our laboratory (Levenson et al., 1999), who showed that resistance to replication-inhibiting drugs in a similar selection protocol required that target cells be co-infected with several different GSEs. Furthermore, one of the members of the GSE combination identified by Levenson et al. was nearly identical with one of the candidate GSEs that was identified in our study and was derived from a mitochondrial gene encoding a subunit of cytochrome c oxidase. Thus, it appears likely that we have isolated some but not all members of a GSE combination that confers resistance to taxol. With this in mind, future studies should include characterization of complete sets of candidate GSEs integrated in single-cell clones obtained after selection, an approach that was used by Levenson et al. (1999) but not in the present study.

On the other hand, the present study has resulted in the development of novel retroviral vectors and methods that should be very useful in future expression-selection studies for both full-length genes and GSEs. These include a series of GFP-expressing retroviral vectors, optimized for co-expression of both GFP and the gene of interest, and the methods for using such vectors to isolate cells co-infected with different viruses and to study changes in the abundance

of cells carrying tested genes or GSEs. Another method developed in the present study is the long-range PCR-based technique for efficient recovery of integrated retroviruses.

Since the results of the present study suggested that a mitochondrially-encoded subunit of cytochrome c oxidase may play a role in cellular drug response, we have developed ρ- sublines of HT1080 cells that are lacking in mitochondrial DNA and characterized changes in the resistance of such sublines to different drugs. We have found that ρ- cells were cross-resistant to several drugs affecting DNA replication; the nature and mechanism of this resistance are under investigation.

Finally, we have found that breast carcinoma cells treated with cytotoxic drugs or retinoids develop phenotypic markers of cell senescence. The expression of such markers is associated with permanent growth arrest in drug-treated cells. Future studies on the mechanisms of drug-induced senescence may open new strategies for augmenting this desirable treatment response in breast cancer.

(10) REFERENCES

Albritton, L.M., Tseng, L., Scadden, D., and Cunningham, J.M. (1989). A putative murine ecotropic retrovirus receptor gene encodes a multiple membrane-spanning protein and confers susceptibility to virus infection. Cell, V.57: 659-666.

Arbuck, S.G., Dorr, A., Friedman, M.A. (1994) Paclitaxel (Taxol) in breast cancer, Hematology/Oncology Clinics of North America, V.8(1):121-140.

Buzdar, A.U., Holmes, F.A., Hortobagyi, G.N.(1995) Paclitaxel in the Treatment of Metastatic Breast Cancer: M.D.Anderson Cancer Center Experience, Seminars in Oncology, V.22(3), Suppl. 6: 101-104.

Chang, B.D., Broude, E.V., Dokmanovic, M., Zhu, H., Ruth, A., Xuan, Y., Kandel, E.S., Lausch, E., Christov, K. and Roninson, I.B. (1999). A senescence-like phenotype distinguishes tumor cells that undergo terminal proliferation arrest after exposure to anticancer agents. Cancer Res. 59, 3761-3767.

Chang, B.D., Xuan, Y., Broude, E.V., Zhu, H., Schott, B., Fang, J., and Roninson, I.B. (1999). Role of p53 and $p21^{waf1/cip1}$ in senescence-like terminal proliferation arrest induced in human tumor cells by chemotherapeutic drugs. Oncogene 18, 4808-4818.

Gudkov, A.V., Kazarov, A.R., Thimmapaya, R., Axenovich, S.A., Mazo, I.A., Roninson, I.B. (1994). Isolation of genetic suppressor elements from a retroviral normalized cDNA library: identification of kinesin associated with drug sensitivity and senescence. Proc. Natl. Acad. Sci. USA, V.91: 3744-3748.

Harris, J.R., Morrow, M., Bonadonna, G. (1993). Cancer of the breast. In: Cancer: Principles and Practice of Oncology, 4th Edition (DeVita, V.T., Hellman, S. and Rosenberg, S.A., eds.), Philadelphia: Lippincott, pp. 1264-1332.

Holzmayer, T.A., Pestov, D.G., Roninson, I.B. (1992). Isolation of dominant negative mutants and inhibitory antisense RNA sequences by expression selection of random DNA fragments. Nucleic Acids Res., V.20: 711-717.

Kandel, E.S., Chang, B.-D., Schott, B., Shtil, A.A., Gudkov, A.V., Roninson, I.B. (1997) Applications of green fluorescent protein as a marker of retroviral vectors. Somat. Cell. Mol. Genet. V.23 (5): 325-340.

Levenson, V.V., Lausch, E. Kirschling, D.J., Broude, E.V., Libants, S., Fedosova, V., and Roninson, I.B. (1999). A combination of genetic suppressor elements produces resistance to drugs inhibiting DNA replication. Submitted to Cancer Res.

Miller, A.D. and Rosman, G.J. (1989). Improved retroviral vectors for gene transfer and expression. Biotechniques. V.7: 980-986.

Roninson, I.B., Gudkov, A.V., Holzmayer, T.A., Kirschling, D.J., Kazarov, A.R., Zelnick, C.R., Mazo, I.A., Axenovich, S., Thimmapaya, R. (1995) Genetic suppressor elements: new tools for molecular oncology. Cancer Res., V.55(18): 4023-4028.

Schott, B., Iraj, E.S., Roninson, I.B. (1996) Effects of infection rate and selection pressure on gene expression from an internal promoter of a double gene retroviral vector. Somatic Cell Mol. Genet., V.22: 292-309.

Schott, B., Kandel, E.S., Roninson, I.B. (1997) Efficient recovery and regeneration of integrated retroviruses. Nucleic Acids Res., V.25 (14): 2940-2942.

Seidman, A.D., Norton, L., Reichman, B.S., Crown, J.P., Yao, T.J., Heelan, R., Hakes, T.B., Lebwohl, DE, Gilewski, TA, Surbone, A, et al.(1993) Preliminary Experience With Paclitaxel (TAXOL) Plus Recombinant Human Granulocyte Colony-Stimulating Factor in the Treatment of Breast Cancer, Seminars in Oncology, V.20(4), Suppl 3: 40-45.

Shen, R., Su, Z.Z., Olsson, C.A., Fisher, P.B. (1995) Identification of the human prostatic carcinoma oncogene PTI-1 by rapid expression cloning and differential RNA display. Proc. Natl. Acad. Sci. U S A. V.92 (15): 6778-6782

(11) PERSONNEL SUPPORTED BY THIS AWARD

Eugene S. Kandel (1995-1998)
Hongming Zhu (1998-1999)

(12) APPENDICES (attached)

- Reprints of three journal articles
- Copies of five meeting abstracts

2940–2942 *Nucleic Acids Research, 1997, Vol. 25, No. 14*

Efficient recovery and regeneration of integrated retroviruses

Brigitte Schott, Eugene S. Kandel and Igor B. Roninson*

Department of Genetics (M/C 669), University of Illinois at Chicago, 900 South Ashland Avenue, Chicago, IL 60607-7170, USA

Received May 21, 1997; Accepted May 27, 1997

ABSTRACT

We report a rapid and efficient PCR-based rescue procedure for integrated recombinant retroviruses. Full-length proviral DNA is amplified by long-range PCR using a pair of primers derived from the long terminal repeats (LTR), and virus is regenerated by transfecting retrovirus-packaging cells with the PCR-derived provirus. The viral yield from the PCR product is similar to that from the retroviral plasmid vector, and the representation of different inserts is accurately maintained in the recovered retroviral population. This procedure is suitable for expression cloning from retroviral libraries and should be applicable to the analysis of natural retrovirus populations.

Retroviral vectors provide one of the most efficient means for gene transfer in mammalian cells. Among other applications, such vectors are used to construct high-complexity libraries for expression cloning of genes (1–3) or genetic suppressor elements (GSEs) (4–6). An integral step in expression cloning is vector recovery from the cells selected for the phenotype of interest; the recovery should be efficient and should adequately reproduce the complexity of the insert sequences present in the selected cells. The usual procedure for the recovery of integrated retroviral vectors involves PCR amplification of inserts from integrated proviruses, which is followed by a labor-intensive step of recloning the PCR products (4). The alternative biological rescue procedures (superinfection with helper virus or fusion with retrovirus-packaging cells) are apt to change the representation of different inserts in the rescued virus population due to differences in virus production by different cells. We have now developed a protocol for rapid and efficient recovery and regeneration of integrated proviruses, which does not require cloning and maintains sequence representation in the recovered virus population. This protocol uses long-range PCR (7,8) to recover functional proviral DNA, which is then used to generate retroviral particles by transient transfection of retrovirus-packaging cells.

The recovery protocol has been developed for the most commonly used type of retroviral vectors based on Moloney murine leukemia/sarcoma viruses and typified by LNCX (9). As illustrated in Figure 1A, the pLNCX plasmid vector contains different 5′ and 3′ LTR sequences; after reverse transcription, both LTR of the integrated provirus acquire the U3 region from the 3′ LTR and the U5 region from the 5′ LTR (10). To amplify the full-length proviral DNA, we have used a sense-oriented (LTRs) primer based on the U3 sequence of the 3′ LTR (5′-AATGAAAGACCCCACCTGTAGGTTTGGCAAGCTAG-3′) and an antisense-oriented (LTRas) primer from the U5 region of the 5′ LTR (5′-CAAATGAAAGACCCCCGTCGTGGGTAGTCAATCAC-3′). Genomic DNA was extracted from retrovirus-transduced cells using Qiagen Blood and Cell Culture DNA kit (high molecular weight and purity of the DNA preparation are critical for the procedure).

Each PCR reaction (50 µl) contained 0.2 mM each of the four dNTPs, 0.5 µg each of LTRs and LTRas primers and 0.5 µg genomic DNA template. In earlier experiments, PCR was carried out in Taq extender buffer (Stratagene) using 10 U *Taq* DNA polymerase (Promega) and 10 U Taq Extender (Stratagene) per tube. In more recent experiments, we have utilized instead TaqPlus Long low-salt buffer and 5 U of TaqPlus Long polymerase mixture (Stratagene); these conditions provided higher and more reproducible PCR yield. PCR was performed in a Perkin Elmer Cetus thermocycler under the following conditions: 3 min at 94°C; 27 cycles of 1 min at 94°C, 1 min at 65°C, and 2.25 min at 72°C; followed by 5 min at 72°C. Figure 1B (lane P) shows the result of a reaction carried out on the DNA from human HT1080 cells transduced with LNCX. The reaction yields two products, a short 0.7 kb band corresponding to the LTR, and a long 4.1 kb band corresponding to the full-length provirus. These conditions have been successfully used to amplify proviral DNA for LNCX or LXSN (9) based vectors (tested with inserts of up to 1.7 kb in the cloning site) in several different types of human cells. In contrast, the same PCR conditions applied to murine cells transduced with the same vectors yielded almost no full-length proviral DNA detectable by ethidium bromide staining, due to cross-reactivity of the LTRs and LTRas primers with LTR of endogenous murine retroviruses. Amplification of proviral DNA from murine cells was made possible, however, by carrying out a second round of PCR on the provirus-size DNA which was gel-purified (without ethidium bromide staining) after the first round of PCR. This is illustrated in Figure 1C, where genomic DNA template was isolated from murine NIH 3T3 cells that were infected with retroviral vector LRSN, which carries an S65T mutant form of the green fluorescent protein (GFP) (11) in the LXSN vector. After the first round of PCR, 15 µl of the reaction were used for electrophoresis in a 1% agarose gel, and DNA was extracted from the region of the gel corresponding to 3.5–4.5 kb, using QIAquick Gel Extraction Kit (Qiagen). 1/3000 of the recovered DNA was used

*To whom correspondence should be addressed. Tel: +1 312 996 3486; Fax: +1 312 413 8358; Email: roninson@uic.edu

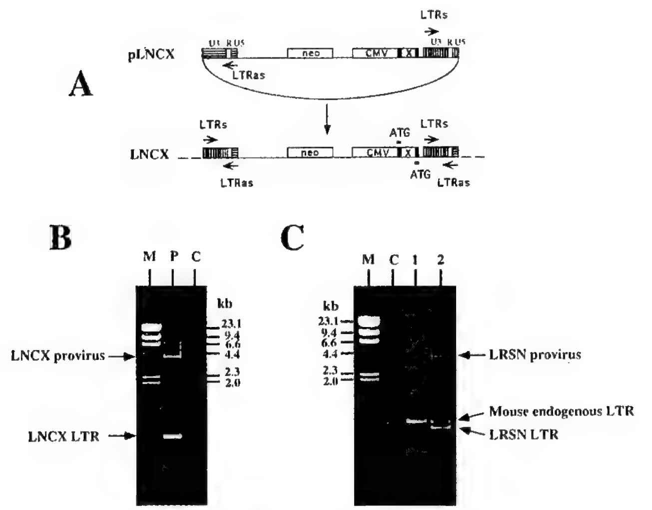

Figure 1. (**A**) Map of LNCX retroviral vector in the form of a plasmid (pLNCX) or integrated provirus. neo, neomycin phosphotransferase gene; CMV, cytomegalovirus promoter; X, insert in the cloning site of the vector. U3, R and U5 indicate the different LTR regions (10). Positions of the primers used for PCR are indicated (LTRs, LTRas, ATG). The 5′ LTR of pLNCX (horizontal stripes) is derived from Moloney murine sarcoma virus, and the 3′ LTR (vertical stripes) from Moloney murine leukemia virus; the origin of the LTR sequences in the provirus is indicated by the corresponding stripes. (**B**) Electrophoretic analysis of a long-range PCR of the DNA from HT1080 cells transduced with the LNCX vector (1% agarose gel). M, size markers (*Hin*dIII-digested λ DNA); P, PCR reaction; C, negative PCR control (no DNA template). (**C**) Electrophoretic analysis of a second round of long-range PCR (see text) of the DNA from NIH 3T3 cells that were uninfected (lane 1) or infected with the LRSN vector (lane 2). Lanes M and C are as in (B).

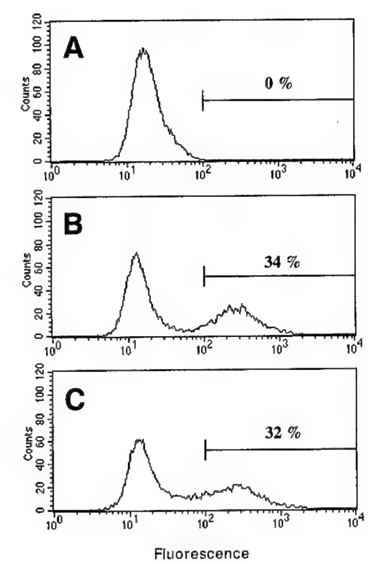

Figure 2. Flow cytometric profiles of HT1080 cells, uninfected (**A**) or infected with retrovirus produced by BOSC23 packaging cells that had been transfected with 1 μg of LRSN supercoiled plasmid vector (**B**) or 1 μg of the PCR-derived LRSN provirus (**C**). 5×10^5 cells were suspended in phosphate buffered saline containing 1 μg/ml propidium iodide (PI). Cells were analyzed with FACSort (Becton-Dickinson) using argon laser excitation (488 nm). PI fluorescence was detected in FL3 emission channel (650LP filter); GFP fluorescence of PI-negative (living) cells was monitored using FL1 emission channel (530/30 BP filter). The data were collected on log scale.

for the second round of PCR under the same conditions. This PCR, when carried out on the DNA from uninfected NIH 3T3 cells, yielded a single band presumably corresponding to the endogenous retrovirus LTR, traces of which remained in the gel-purified sample. In contrast, genomic DNA from LRSN-infected cells yielded bands corresponding to the endogenous and vector-derived LTR, as well as a full-length 4.1 kb LRSN provirus (lane 2).

PCR-amplified proviral DNA (combined with salmon sperm carrier DNA to a total of 15 μg) was used to transfect BOSC 23 ecotropic retrovirus-packaging cells (12); the transfection and subsequent infection of recipient cells were carried out as previously described (13). In some experiments, PCR-amplified LNCX-based provirus, recovered from HT1080 cells by a single round of PCR, was purified using QIAquick PCR Purification Kit (Qiagen) and products of one to five PCR reactions were used for transfection. Infected cells were obtained under these conditions, but at a relatively low (<3%) rate. To maximize the viral yield from the provirus derived by a single round of PCR, we gel-purified proviral DNA from a mixture of 20 PCR reactions prior to transfection (without ethidium bromide staining). The efficiency of infection with the LRSN virus recovered under these conditions and the ability of this virus to express functional GFP and Neo proteins were evaluated either by the percentage of fluorescent cells expressing GFP (as measured 3 days after infection) or by the formation of G418-resistant colonies. Figure 2 shows the fluorescence profiles of HT1080 cells (expressing the murine ecotropic receptor, 14) that were either uninfected or infected with retrovirus produced by BOSC23 cells after transfection with

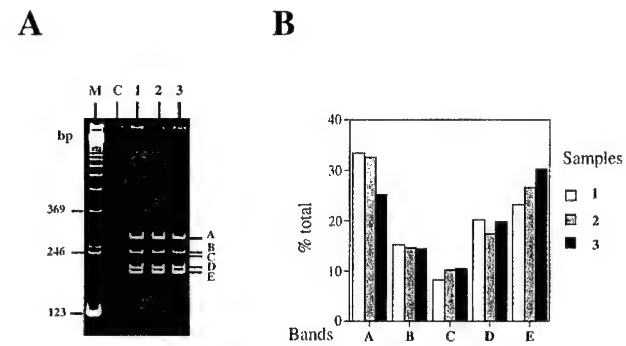

Figure 3. Short-range PCR analysis of representation of different-size inserts in a population of LNCX-derived proviruses. The following templates were used for PCR: genomic DNA of HT1080 cells carrying the integrated provirus population (sample 1), proviral DNA recovered from the same cells by long-range PCR (sample 2), genomic DNA from HT1080 cells transduced with the rescued provirus population (sample 3). Five distinct inserts are designated A–E. (**A**) Electrophoretic analysis of the PCR products in 6% polyacrylamide gel. M, size standards (123 bp ladder); C, negative PCR control (no DNA template). (**B**) Relative intensity of bands A–E in samples 1–3, as measured in ethidium bromide-stained polyacrylamide gel using ISO 1000 gel imaging system (Alpha Innotech). The intensity of each band is represented as the percentage of total intensity of all five bands for a given sample.

1 μg of LRSN plasmid DNA or the same amount of gel-purified LRSN proviral DNA. The percentage of cells infected with the plasmid-derived virus was 34% by fluorescence and 30% by G418 resistance, while the corresponding values for the recovered virus were 32 and 46%, indicating that the PCR-generated linear provirus was transcribed in BOSC23 cells as efficiently as the supercoiled plasmid. In the case of LRSN recovered from murine

NIH 3T3 cells by two rounds of PCR, the product of a single PCR reaction (purified using QIAquick PCR Purification Kit) yielded the infection rate of 7.6% by fluorescence and 10% by G418 resistance (data not shown).

The maintenance of sequence representation in the recovered retrovirus population is illustrated by an experiment carried out on HT1080 cells that were infected with a normalized cDNA fragment library in the LNCX vector and selected for resistance to taxol (E.S.K., unpublished). The cDNA inserts from retroviral vectors integrated in this subpopulation were amplified by PCR using a primer (ATG) corresponding to the adaptor sequence flanking the inserts (5). Figure 3A shows electrophoretic analysis of PCR products amplified directly from genomic DNA, from full-length proviral DNA recovered by long-range PCR, or from genomic DNA of HT1080 cells infected with the recovered provirus and analyzed 3 days after infection. Each lane contains five distinct bands; their relative intensity is shown in Figure 3B. The representation of different bands is very similar in all three lanes, indicating that sequence representation in this relatively simple population has been maintained throughout the procedure.

In summary, the described provirus recovery protocol is rapid (3 days from genomic DNA extraction to the generation of infectious virus), effficient, and capable of maintaining sequence representation in the retroviral population. This protocol should be useful not only for expression cloning in retroviral vectors but also for functional analysis of sequence variability of full-length genomes in naturally occurring 'quasispecies' of different retroviruses (including HIV).

ACKNOWLEDGEMENTS

We thank Elizabeth S.Iraj for technical assistance, Donald Zuhn and Andrei Gudkov for helpful discussions, and Randal Cox for help with the illustrations. Supported by US National Cancer Institute grants R01-CA56736 and R01-CA62099, US Army grant DAMD17-94-J-4038 (I.B.R.) and US Army predoctoral fellowship DAMD17-96-I-6050 (E.S.K.).

REFERENCES

1 Murphy,A.J.M. and Efstratiadis,A. (1987) *Proc. Natl. Acad. Sci. USA* **84**, 8277–8281.
2 Rayner,J.R. and Gonda,T.J. (1994) *Mol. Cell. Biol.* **14**, 880–887.
3 Kitamura,T., Onishi,M., Kinoshita,S., Shibuya,A., Miyajima,A. and Nolan,G.P. (1995) *Proc. Natl. Acad. Sci. USA* **92**, 9146–9150.
4 Gudkov,A.V., Zelnick,C.R., Kazarov,A.R., Thimmapaya,R., Suttle,D.P., Beck,W.T. and Roninson,I.B. (1993) *Proc. Natl. Acad. Sci. USA* **90**, 2131–3235.
5 Gudkov,A.V., Kazarov,A.R., Thimmapaya,R., Axenovich,S.A., Mazo,I.A. and Roninson,I.B. (1994) *Proc. Natl. Acad. Sci. USA* **91**, 3744–3748.
6 Ossovskaya,V.S., Mazo,I.A., Chernov,M.V., Chemova,O.B., Stresoska,Z., Kondratov,R., Stark,G.R., Chumakov,P.M. and Gudkov,A.V. (1996) *Proc. Natl. Acad. Sci. USA* **93**, 10309–10314.
7 Barnes,W.M. (1994) *Proc. Natl. Acad. Sci. USA* **91**, 2216–2220.
8 Cheng,S., Fockler,C., Barnes,W.M. and Higuchi,R. (1994) *Proc. Natl. Acad. Sci. USA* **91**, 5695–5699.
9 Miller,D.A. and Rosman,G.J. (1989) *Biotechniques* **7**, 980–986.
10 Luciw,P.A. and Leung,N.J. (1992) In Levy,J.A. (ed.), *The Retroviridae 1*. Plenium press, New York and London, chap. 5, pp. 159–263.
11 Heim,R., Cubitt,A.B. and Tsien,R.Y. (1995) *Nature* **375**, 663–664.
12 Pear,W.S., Nolan,G.P., Scott,M.L. and Baltimore,D. (1993) *Proc. Natl. Acad. Sci. USA* **90**, 8392–8396.
13 Schott,B., Iraj,E.S. and Roninson,I.B. (1996) *Somatic Cell. Mol. Genet.* **22**, 292–309.
14 Albritton,L.M., Tseng,L., Scadden,D. and Cunningham,J.M. (1989) *Cell* **57**, 659–666.

Somatic Cell and Molecular Genetics, Vol. 23, No. 5, 1997, pp. 325–340

Applications of Green Fluorescent Protein as a Marker of Retroviral Vectors

Eugene S. Kandel, Bey-Dih Chang, Brigitte Schott, Alexander A. Shtil, Andrei V. Gudkov, and Igor B. Roninson

Department of Molecular Genetics, University of Illinois at Chicago, 900 South Ashland Avenue, Chicago, Illinois, 60607–7170

Received 12 December 1997—Final 12 December 1997

Abstract—*The Green Fluorescent Protein (GFP) of* Aequorea victoria *is used as a vital fluorescent tag for the detection and isolation of genetically modified cells. Several modified variants of GFP were tested as marker genes in retroviral vectors containing different backbones and promoter combinations. Constructs allowing for reliable detection of GFP fluorescence and the expression of a cotransduced gene from a strong promoter were identified. Cells harboring such constructs are detectable by flow cytometry, fluorescence microscopy and multi-well fluorescence reading. GFP expression in transduced cells is stable both in vitro and in vivo, and long-term dynamics of GFP-positive fractions in a mixed population can be used to monitor the biological effects of a cotransduced gene. Selection of cells with the highest GFP fluorescence enriches for multiply infected cells. The use of different GFP variants allows one to monitor simultaneously two cell populations transduced with vectors carrying GFPs that differ in their fluorescence intensity or spectral properties and to identify doubly transduced cells. In addition, transcription of an inducible promoter positioned in the opposite orientation to GFP can be monitored by the inhibition of GFP fluorescence. Thus, GFP provides a useful marker for gene transfer by retroviral vectors and extends the range of applications for retroviral transduction.*

INTRODUCTION

Retroviral transduction provides one of the most efficient and convenient means of gene delivery into animal cells. Benefits of this method include a broad spectrum of target cell types, stable integration of a transgene, predictable structure of an integrated construct and many more. Its applications extend beyond in vitro experimentation, and are being explored clinically for gene therapy. However, infection efficiency of the target cells rarely reaches 100%. Hence, for most experimental purposes it is necessary to determine the fraction of infected cells and, in many cases, obtain a pure population of infectants. For this reason, the gene of interest is usually introduced in a construct that also carries a marker gene that provides an identifiable and selectable phenotype.

The most popular class of markers consists of genes that confer resistance to various cytotoxic compounds, so that non-transduced cells can be eliminated in the course of an appropriate selection. While numerous markers of this type are available, they all share some common disadvantages. First, the efficacy of selection differs depending on the target cells and the conditions of their culture, so that the selection protocol should be optimized for each

0740-7750/97/0900-0325$12.50/0

cell/drug combination. Second, in many cases the exposure to cytotoxic agents is undesirable, since it may affect the cell behavior in subsequent experiments. Third, it takes from several days to several weeks for a complete drug selection to occur. Fourth, the requirement for continuous expression of the drug resistance gene may favor cells that inactivated the transcription unit encoding the gene of interest, due to competition between the promoters driving this transgene or the drug resistance gene. As a result, in some cases the transduced population can be completely overgrown by clones that fail to express a transgene (1).

A recently introduced marker gene for Green Fluorescent protein (GFP) from *Aequorea victoria* (2) provides an attractive possibility to circumvent these and other limitations of conventional selectable markers. This naturally fluorescent protein (peak excitation at 376 nm, emission at 510 nm) retains fluorescence when expressed in a heterologous host. Several altered-fluorescence variants of GFP have been developed. So called "red-shifted" (488 nm excitation, 510 nm emission) variants of GFP are of particular promise, as they may be detected and isolated using the most common equipment for flow cytometry optimized to monitor fluorescein isothiocyanate (FITC) (3, 4). "Blue-shifted" (UV excitation, blue light emission) variants of GFP, "Blue Fluorescent Proteins" (BFPs), have also been developed (5–7). Due to their different spectra "red-shifted" and "blue-shifted" proteins can be detected simultaneously, although BFP requires less common detection optics.

Several groups have reported earlier successful transfer of genes for some forms of GFP through retroviral transduction (8–11). A limitation of these studies is that most of the described constructs were optimized specifically for GFP expression, while a possibility to use GFP as a marker for transduction of other genes was suggested but not explored in detail. While these groups reported no specific problems with retroviral transduction of GFP, Hanazono et al. (12) encountered difficulties in establishing high-titer producing cell lines based on PA317 packaging cells and suggested that GFP may have a cytotoxic effect and "may not be an appropriate reporter gene for gene transfer applications" (12). We have now designed, constructed and tested an extensive series of retroviral vectors that express different forms of GFP. We have compared these constructs and developed several novel applications for GFP as a marker for gene delivery, detection, isolation and characterization of cells infected with retroviral vectors.

MATERIALS AND METHODS

Plasmids and Cell Lines. LNCX and LXSN (13) were kindly provided by Dr. A.D. Miller. pBabeBleo (14) was a gift of Dr. H. Land. IPTG-regulated vectors LNXCO3, LNXCO4 and LNXRO2 were previously described (15). cDNA for the wild type GFP, GFP S65T, EGFP, EBFP was derived from pGFP1, pGFPS65T-C1, pEGFP-C1, and pEBFP-C1 plasmids, respectively (Clontech, Inc). pGreenLantern1 (Gibco BRL) was used as the source of "GreenLantern" cDNA. A mutant version of MoMuLV/MoMuSV LTR (16) was synthesized and kindly provided by Dr. W. Chen. Plasmid pCMV-P53 containing a cDNA for wild-type human tumor suppressor p53 was a gift of Dr. P. Chumakov. Details of plasmid construction are available upon request.

Bosc23 ecotropic packaging cell line (17) was a gift of Drs. W. Pear and D. Baltimore. HT1080-E14 cell line was derived by us from HT1080 human fibrosarcoma cell line after stable transfection with pBabeBleo vector (14) expressing the cDNA for murine ecotropic receptor (18). HT1080-3′SS6 is a derivative of HT1080-E14 expressing a modified LacI repressor (15). All the cells were grown in DMEM with 10% fetal calf serum at 37°C and 7% CO_2.

Transfection and Retroviral Transduction. Plasmid DNA was prepared using Qiagen Plasmid Maxi Kit (Qiagen, Inc.) according to the manufacturer instructions. Transfection of Bosc23 packaging cells was carried out as

described (17) using 10–20 μg of plasmid DNA. Target cells were plated at a density of 1–2 × 10^5 cells per P100 tissue culture plate one day before infection. The supernatant of transfected Bosc23 cells was collected 36 hrs after transfection, filtered through 0.45 nm SFCA filter (Nalgene) and added to the target cells in the presence of 4 μg/ml polybrene. When indicated, the viral stock was diluted with the growth medium. After an overnight incubation, the viral supernatant was replaced with a fresh medium.

G418 selection of infectants was carried out in the presence of 0.4 mg/ml G418 with media change every 3–4 days, until complete cell killing was observed in a non-infected control plate treated in parallel.

FACS Analysis and Cell Sorting. Cells were harvested by brief trypsinization, washed with phosphate-buffered saline (PBS) and resuspended in PBS to the final concentration of 10^5–10^6 cell per ml. FACS analysis of wild-type and red-shifted GFP variants for individual experiments has been performed using one of the three flow cytometers: FACSort, FACSVantage (both with argon laser excitation at 488nm, GFP detection using BP530/30 filter; Becton Dickinson) and Coulter Epics Elite (argon laser excitation at 488nm, GFP detection using BP525/10 filter). Propidium iodide (PI) was added to the samples to the final concentration of 1 μg/ml and PI fluorescence was used to distinguish between live and dead cells. Only live (PI-negative) cells with normal morphology (as determined by side and forward scatter) were included in the analysis. Typically 1–2 × 10^4 viable cells were analyzed. Similar results were obtained using either one of the three machines.

Simultaneous flow cytometric analysis of LNCB and LXSE infected cells was carried out with a modified Coulter Epics 753 flow cytometer. Cells were excited with blue (488nm band) and UV (predominantly 351nm and 363nm bands) light. Light from the sample first passed through a UV laser block (408LP filter). 10% reflecting mirror was used to direct light through a standard 488 band pass filter to a side scatter detector. For the passing light, 490LP dichroic mirror was used to direct shorter blue light through a 440/40BP filter for the detection of EBFP fluorescence, while the light of longer wave length was transmitted to 550LP dichroic mirror. Reflected green light was passed through 525/10BP filter and used to measure EGFP fluorescence, while transmitted red light was passed through 635/10 BP filter and used to detect propidium iodide fluorescence.

Cell sorting was carried out using FACS-Vantage under the conditions described above. Sorted cells were collected in DMEM with 20% fetal calf serum. Subsequently, cells were pelleted, resuspended in regular growth medium and plated on tissue culture plates. For the establishment of single cell subclones, selected cells were directly deposited onto 96-well tissue culture plates using a cell deposition unit.

Detection of GFP Expression by Fluorescence Microscopy and Multi-well Fluorescence Reading. For fluorescence microscopy cells were trypsinized, washed with PBS and deposited on microscopic slides. The microscopes used were: Nikon Labophot-2 fluorescent microscope with XC75 CCD video camera (Nikon) and DAPI (for BFP detection) or FITC (for red-shifted GFP) filter sets, and Leitz fluorescent microscope with FITC filter set (for detection of wild-type and red-shifted GFP). We have also used Olympus epifluorescent microscope with RF-2 module and FITC filter set to visualize GFP expression in cells attached to the tissue culture plates.

For GFP detection in a multi-well format, cells were seeded onto 24-well tissue culture plates (Falcon). Prior to measurement, the growth medium was substituted with PBS and the fluorescent signal was read using CytoFluor II multi-well plate reader (Perseptive Biosystems) using 485 nm excitation and 530nm emission filter sets.

Copy Number Analysis of the Integrated Proviruses. Individual cell clones were expanded and genomic DNA was extracted using Qiagen Blood and Cell Culture DNA kit (Qiagen) according to the manufacturer's recommendations. DNA was digested with KpnI.

Following digestion, DNA was purified and its concentration was measured using diphenylamine method, in triplicates for each sample. 10 μg of each sample was loaded on 0.8% agarose gel along with KpnI-digested calibration mixtures of DNA of non-infected cells and pLXSE plasmid, prepared at the ratios corresponding to 1 and 2 copies of pLXSE per diploid amount of DNA. Upon electrophoresis, samples were transferred onto HybondN (Amersham) nylon membrane. The NheI/BglII fragment of pEGFP-C1 containing the cDNA of EGFP was used as a probe after labeling with ^{32}P by random priming using the Multiprime DNA Labeling System (Amersham). Hybridization and high-stringency washing were carried out as previously described (19). To determine the provirus copy number in test samples, radioactive signal from individual bands was quantified using Betascope 603 Blot Counter (Betagen Corp.) and divided by the signal generated by the pLXSE plasmid in the calibration mixtures.

RESULTS AND DISCUSSION

Comparison of GFP-Expressing Retroviral Vectors. The retroviral backbones in our constructs have been derived from the earlier published vectors (13–15). We originally started by cloning the wild-type GFP cDNA from pGFP1 plasmid (Clontech, Inc) into LNCX (13) retroviral vector. The resulting pLNCGfp plasmid was used to transfect Bosc23 packaging cells (17) and the viral supernatant was used to infect murine NIH3T3 fibroblasts and human HT1080-E14 fibrosarcoma cells. Transfected and infected cells were analyzed using fluorescent microscopy or flow cytometry under conditions optimized for the detection of FITC. In neither case were we able to detect fluorescent signal (data not shown), suggesting that the wild-type GFP was not efficiently excited by the blue light in our available equipment.

Various "red-shifted" GFP variants gradually became available over the course of this study. GFP S65T (from pS65T-C1; Clontech) contains an amino acid substitution that brings excitation peak of this protein close to 488 nm, a property ideally suited for detection using conventional argon lasers as well as other equipment developed for the detection of FITC. In addition, GFP S65T was reported to have improved folding rate of the chromophore, as compared to the wild type GFP. "Green Lantern" GFP (from pGreenLantern1; GIBCO BRL) contains the same S65T mutation, as well as optimization of certain codons in order to avoid those that are particularly unfavorable for translation in human cells (20). "Enhanced GFP" or "EGFP" (21) (from pEGFP-C1, Clontech) was engineered to include S65T change as well as complete optimization ("humanization") of the codons and additional mutations (22) that improve folding and reduce aggregation. In addition to the red-shifted variants, we have also used BFP (from pEBFP-C1, Clontech) which contains the Y66H mutation that changes the fluorescence spectrum (5–7) together with mutations improving folding and chromophore formation (22), as well as complete "humanization" of the coding region.

Figure 1 shows the structures of different GFP-containing retroviral vectors that we generated, as well as their relative fluorescence (RF) values, determined after retroviral transduction into derivatives of HT1080 cells. Since the most important characteristic of a fluorescent marker is the separation achieved between positive and negative cells, the RF is defined as a ratio between median fluorescence of GFP-positive and GFP-negative cells. The absolute fluorescence, as measured by FACS, may change depending upon the setup of the instrument (e.g. laser power or amplification parameters for the detectors). However, the RF of FACS-distinguishable distinct cell populations remains essentially the same regardless of the changes in the absolute values. This allows us to compare results obtained using the same FACS with the same cell line, but at different times. The use of median, rather than mean, fluorescence values makes RF relatively insensitive to the appearance of rare particles with abnormal fluorescence as well as to minor experimental varia-

Vector structure	Name	Relative Fluorescence
LTR NEO CMV S65T LTR	LNCR	10-20
LTR S65T SV40 NEO LTR	LRSN	10-30
LTR S65T CMV LTR	LRCX	2-3
LTR CMV S65T LTR	LXCR	10-20
LTR NEO CMV G.L. LTR	LNCG	100-200
LTR SV40 G.L. LTR	LXSG	15-20
LTR G.L. CMV LTR	LGCX	7
mLTR G.L. CMV mLTR	LmGCX	8-10
LTR NEO CMV EGFP LTR	LNCE	200-600
LTR SV40 EGFP LTR	LXSE	20-40
LTR EGFP CMV LTR	LECX	10
mLTR EGFP CMV mLTR	LmECX	12-15
LTR EGFP SV40 LTR	LESX	50-65
LTR SV40 EGFP LTR	BabeE	20
LTR NEO PGK EGFP LTR	LNPE	10-20
mLTR EGFP mLTR	LmEX	150
LTR NEO CMV EBFP LTR	LNCB	N.A.
LTR SV40 EBFP LTR	LXSB	N.A.
LTR G.L. A RO2 LTR	LGXRO2	20
LTR G.L. A CO3 LTR	LGXCO3	8
LTR G.L. A CO4 LTR	LGXCO4	8

Fig. 1. Structures and relative fluorescence values of GFP-containing retroviral vectors. Vectors are shown as integrated proviruses. Relative fluorescence (RF) was determined in HT1080 cells transduced with the corresponding viruses, using excitation with an argon laser on Becton Dickinson FACSort flow cytometer (EBFP is not fluorescent under these conditions). RF for LGXRO2, LGXCO3 and LGXCO4 was determined in the absence of β-galactosides. A range of RF is shown for the most extensively tested vectors. LTR—Moloney Murine Leukemia/Sarcoma Virus Long Terminal Repeat; mLTR—modified LTR with an extra Sp1 binding site (16); CMV—human cytomegalovirus promoter/enhancer region; SV40—Simian Virus 40 promoter/enhancer region; PGK—murine phosphoglycerate kinase gene promoter; RO2—modified Rous Sarcoma Virus Long terminal Repeat with 2 *lac*-operators (15); CO3,CO4—modified CMV promoters with 3 and 4 *lac*-operators respectively (15); neo—neomycin phosphotransferase gene; S65T—GFP S65T from pS65TC1 (Clontech); G.L.—"Green Lantern" GFP from pGreenLantern (Gibco BRL); EGFP—"Enhanced GFP" from pEGFPC1 (Clontech); EBFP—"Enhanced Blue Fluorescent Protein" from pEBFP (Clontech); X—proposed cloning sites (vary from vector to vector); A—polyadenylation signal from Herpes Simplex Virus thymidine kinase gene.

tions in gating. For a given construct, the RF may be affected by several factors. One of them is autofluorescence of uninfected cells, which in its turn is affected by culture conditions and the diluent used to prepare cells for analysis (e.g. growth medium or PBS). Only the results obtained in PBS were included in Fig. 1. The second factor that influences RF is the infection rate. Populations infected at higher rates exhibit higher median fluorescence, probably as a result of multicopy integration (as shown below). For this reason, results obtained at infection rates higher than 50% were generally excluded from the table. Another parameter affecting RF is the length of time in culture from infection to analysis. We have observed that maximal RF is achieved between 48 and 72 h after infection, although fluorescent cells can be detected much earlier. Hence, Fig. 1 contains data only from analysis done 48 or more hours post infection. For the most extensively analyzed constructs, a typical range of RF is given. RF values presented in this paper were obtained using argon laser excitation (488nm). BFP is not fluorescent under these conditions, but, as described below, it was detectable by flow cytometry with UV excitation or fluorescent microscopy. Comparison of the RF values for red-shifted GFP variants in similar retroviral backbones yielded the following hierarchy: EGFP > "Green Lantern" > GFP S65T (compare LNCR to LNCG and LNCE; Fig. 1). While this article was in preparation, similar ranking of GFP variants (EGFP > "humanized" GFPS65T, "red-shifted" GFP > wtGFP) was reported by others (23).

The other major determinant of RF is the promoter which drives GFP expression. We consistently observed high levels of GFP expression from the human CMV promoter, as determined both by FACS and fluorescent microscopy. In fact, we faced an unexpected problem when doing FACS analysis on cells infected with the LNCE vector (Fig. 1): due to extremely high fluorescence level, positive cells were hard to analyze on the same scale with the uninfected cells. This high fluorescence level allows us to identify unambiguously and isolate cells that are infected or transfected with such vectors, even when such cells comprise only a fraction of a percent in the total population.

Somewhat lower level of expression was observed from the vectors in which GFP expression was driven by the SV40 promoter (compare LNCG to LXSG and LNCE to LXSE; Fig. 1). Noteworthy, we observed a small but detectable decrease in fluorescence provided by LXSE carrying an insertion in its cloning sites, but this decrease did not jeopardize FACS-based detection of transduced cells (data not shown). This observation suggests, however, that when a drug resistance gene rather than GFP is used as a selectable marker, the expression of this gene and hence the toxicity of the selective agent may be different for cells transduced with insert-containing and insert-free vectors. Thus, a vector containing a biologically inert insert may be a more accurate negative control than an insert-free vector, unless GFP is used as a selectable marker.

The murine phosphoglycerate kinase (PGK) promoter provided only a low fluorescence in the LNPE construct (Fig. 1). However, the PGK promoter is known to be stably expressed in a very broad variety of murine tissues (24), and therefore in some cell types it might be more useful than in HT1080 cells.

We were especially interested in developing GFP vectors analogous to a commonly used neo-containing vector LNCX (13), where the potent CMV promoter would drive the expression of the non-selected gene of interest, while GFP would be expressed from the LTR promoter. We have encountered considerable difficulties, however, in using LRCX vector, the first vector of this type, where the RF of the S65T GFP turned out to be substantially lower than in any other construct tested (Fig. 1); LRCX-transduced cells were essentially indistinguishable from their non-infected counterparts. We have tried three different cloning strategies to obtain a functional vector of LRCX structure,

and numerous individual plasmid clones were analyzed (data not shown), yet none of the constructs yielded sufficient fluorescence for our applications. We cannot attribute this to an insufficient activity of the LTR promoter per se, since LRSN vector containing the same LTR-GFP cassette but carrying SV40 rather than CMV as the internal promoter provides relatively strong fluorescent signal (Fig. 1). Similarly, the LESX vector carrying EGFP has provided much brighter signal than LECX (Fig. 1). Our results suggest that the CMV promoter interferes with LTR-driven expression of GFP (compare LmECX to LmEX; Fig. 1). This is in agreement with our previous observations that G418 selection of cell populations infected with an LNCX-based vector leads to the accumulation of cells with inactivation of the CMV-driven gene (1). Despite the failure of LRCX, its analogs carrying improved versions of GFP, LGCX and LECX, provided acceptable levels of RF. These levels were further improved by the use of a mutant version of MoMuLV/MoMuSV LTR, which contains a new Sp1 site in its U3 area (16), in the LmGCX and LmECX vectors (Fig. 1). These vectors allow one to take advantage of the strong CMV promoter for the expression of the gene of interest.

Aside from the above-described vectors based on the LN retroviral backbone (13), we have also inserted GFP into pBabe vector backbone (14). Vectors of pBabe series carry a variety of resistance markers as well as some modifications for improved virus packaging. We have modified pBabeBleo to incorporate EGFP in place of *bleo*. The resulting construct, pBabeE, is similar to the LN-based pLXSE vector, yielding similar titer of infectious virus (not shown) as well as fluorescence of infected cells (Fig. 1). The pBabeE plasmid is smaller than pLXSE and is based on a higher copy replicon that simplifies manipulations with this vector in plasmid form. In addition, the availability of both pLXSE and pBabeE extends cloning options by providing two vectors with similar structure but different sets of restriction sites.

The observations summarized in Fig. 1 suggest some possibly general predictions for gene expression from retroviral vectors expressing one gene from the LTR and the second from an internal promoter in the same orientation. While these predictions are based primarily on the results obtained in human fibrosarcoma cells, they are in agreement with our observations in a number of other cell types, including murine and rat fibroblasts and human breast carcinoma cells (unpublished observations). First, vectors containing an internal SV40 promoter are likely to express both genes at similar levels (compare LXSE to LESX). Thus, such vectors as LXSG, BabeE, LXSE, LESX and LXSB are well balanced in terms of relative expression of both transcriptional units. In contrast, vectors carrying an internal CMV promoter would probably favor very high expression of the downstream gene but relatively low of the upstream gene (compare LRCX to LXCR and LECX to LNCE). We suggest that LGCX, LmGCX, LECX and LmECX would be the vectors of choice when the highest expression level of the CMV-driven gene of interest is desired, while the ease of detection of GFP-expressing cells is not a priority. In contrast, LNCG, LNCE and LNCB may be used (after substituting *neo* for the fragment of interest) when it is desired to have the highest possible fluorescence, although transgene expression from LTR may be lower than from the CMV promoter.

Long-Term Stability of GFP Expression. To investigate whether GFP expression from our vectors would have any detrimental effect on cell viability or proliferation, we infected a population of HT1080-E14 cells with LNCG virus and continuously propagated the infected population in the absence of any selection. The composition of the population in respect to GFP fluorescence was periodically determined by FACS. After more than three months of culture (>115 cell doublings) the fraction of GFP-positive cells sustained only minor changes (Fig. 2A) while the relative fluorescence of the positive cells remained essentially the same

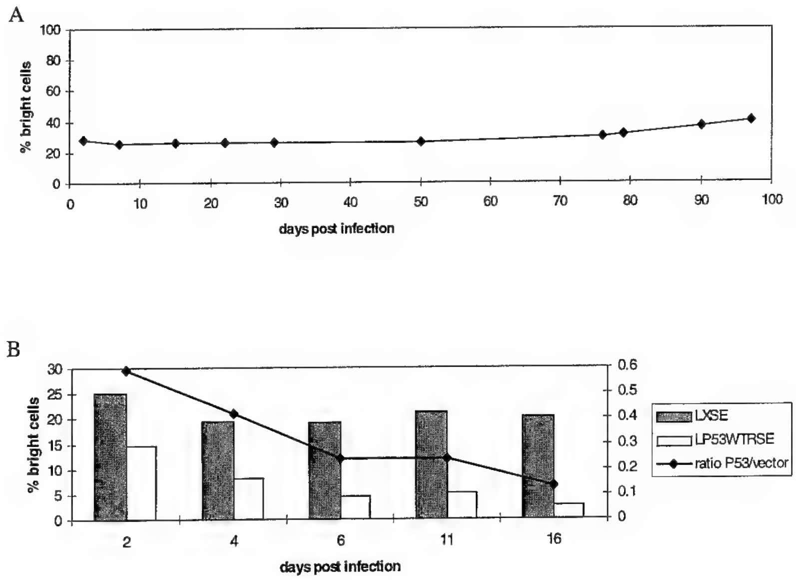

Fig. 2. GFP stability in transduced cells. Panel A. Long-term stability of GFP-positive fraction in a mixed population. HT1080-E14 cells infected with LNCG virus from Bosc23 packaging cells were continuously propagated in the absence of selection. The percent of GFP-positive cells was periodically determined by FACS analysis. Panel B. Demonstration of the growth-inhibitory effect of p53 tumor suppressor through changes in the GFP-positive fraction. HT1080-3′SS6 cells were infected in parallel with either LXSE or LP53WTRSE (wild type p53 cDNA in LXSE vector) virus, in duplicates. The percent of GFP-positive cells was periodically assayed by FACS analysis. Standard errors for the duplicates were <10% of the mean in all cases. The decreasing ratio of the fractions of GFP-positive cells between LP53WTRSE and LXSE demonstrates a gradual loss of infected cells in which GFP was cotransduced with the tumor suppressor.

(data not shown). Similar observations were made with several other cell types infected with GFP vectors (20–30 days monitoring), including murine NIH 3T3 and rat Rat1 fibroblasts, and MCF7 human breast carcinoma cells (E.S.K., B.S., Y. Xuan, and I.B.R., unpublished).

To test the stability of coexpression of GFP and a cotransduced gene, we infected HT1080-E14 cells with LNCR virus, yielding a 9% GFP-positive population. Subsequently, one part of the infected population was selected for *neo* gene function by growth in the presence of G418. FACS analysis of the resistant cells was carried out upon completion of selection (10 days post infection), and revealed >93% GFP-positive cells. The other part of the population was used after infection to isolate GFP-positive cells by FACS sorting, after which GFP-positive cells were assayed for colony formation in the presence and in the absence of G418. Sorted cells remained almost 100% positive for GFP upon reanalysis two weeks after sorting and their plating efficiency with and without G418 was essentially the same, indicating close to 100% positivity for *neo* expression.

To verify that GFP does not interfere with cell growth in vivo and is detectable within a tumor, we injected a mixture of HT1080-E14 cells, both non-infected and infected with LNCG, subcutaneously into a nude mouse. Three weeks later, the growing tumor was excised and pieces of it were viewed under a fluorescent microscope. As expected, the specimen represented a mixture of fluorescent and non-fluorescent cells (Fig. 3, A and B). A part of a tumor was trypsinized and plated in tissue culture. After one passage in culture, recovered cells were subjected to FACS analysis revealing presence of GFP-positive cells with characteristically bright fluorescence (Fig. 3C). Thus, GFP-expressing cells can be readily identified

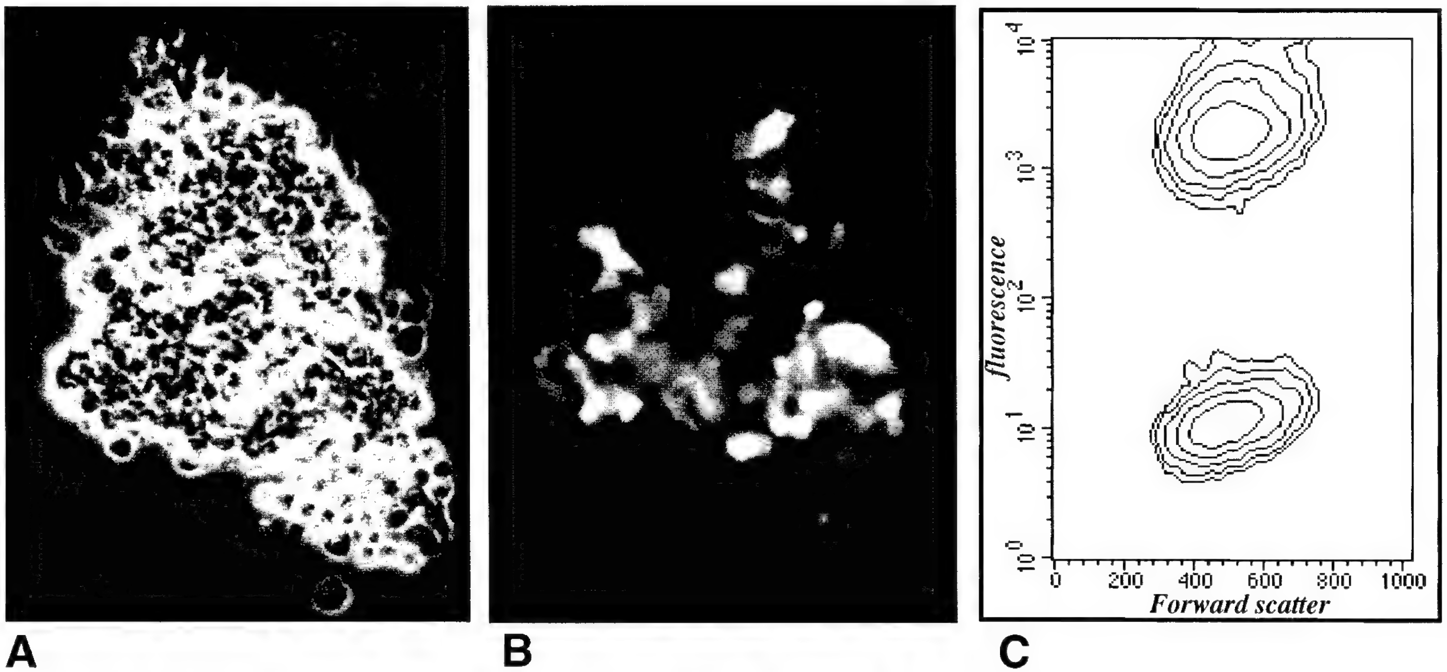

Fig. 3. GFP expression does not interfere with tumorigenicity and is detectable in tumors grown in vivo. HT1080 cells were infected with LNCG virus and expanded without selection. 2×10^6 cells were subcutaneously injected into a nude mouse. Three weeks later the tumor was removed and analyzed under a Leitz fluorescent microscope in a bright field (A) or with FITC filter set to detect GFP fluorescence (B). A part of the tumor was trypsinized and explanted in cell culture. After one passage in culture the cells were analyzed by FACS, revealing the retention of a bright fluorescent population (C). Results of the flow cytometric analysis are shown on the contour plot of fluorescence versus forward scatter with 2% threshold and one smoothing iteration.

within tumors and recovered for subsequent manipulations.

The above results indicate that GFP expression is stable both in vitro and in vivo and has no detrimental effect on cell growth. Our observation of the stability of GFP expression in vivo is in agreement with the reports that GFP transgenic animals are viable and lack signs of major abnormalities (25). Furthermore, stable production of a GFP-containing retroviral vector has been successfully achieved in PA317 cells (9), suggesting that the reported failure of GFP expression in this cell line (12) is unlikely to be due to the GFP toxicity. Although we cannot exclude that extremely high expression of GFP, as of almost any protein, may be detrimental to a cell, we believe that inability to obtain stable GFP-expressing cells is more likely to result from inadequate expression, selection or detection systems.

Use of GFP to Monitor Growth Effects of a Cotransduced Gene. Given the stability of GFP expression, we hypothesized that changes in the GFP positive population may serve as a sensitive indicator of the effects of a cotransduced gene on cell growth. To test the applicability of GFP to monitor cellular effects of a tumor suppressor gene, we infected HT1080–3′SS6 cells with LP53WTRSE (wild type p53 cDNA in LXSE vector) or with insert-free LXSE vector and monitored FACS profiles of the infected populations (in duplicates) over a period of 16 days. We have observed a gradual decrease in GFP-positive cells when GFP was cointroduced with p53 (from ~15% at day 2 to ~2% on day 16), while the fraction of GFP positive cells infected with the LXSE control remained essentially unchanged (Fig. 2B). This phenomenon was reproduced in a number of similar experiments that differed in the initial transduction rate (10–95%) and duration of observation (16–28 days) (data not shown). Thus, periodic monitoring of the GFP-positive fraction in the infected cell population should provide a convenient and sensitive means to detect the effects of different

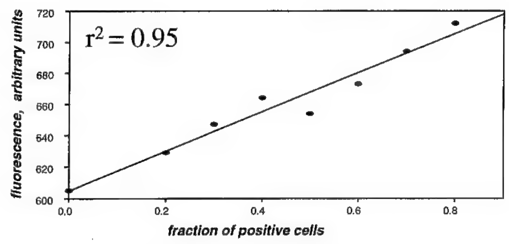

Fig. 4. Detection of transduced cells using a multi-well fluorescence plate reader. Different numbers of HT1080-3′SS6 cells transduced with LNCG virus and selected with G418 were added to non-infected cells to produce mixtures of various composition. For each mixture, two wells of a 24-well cell culture plate were seeded with 50,000 cells. The next day the growth medium was substituted for PBS and the fluorescent signal was read on CytoFluor II multi-well fluorescence plate reader (Perseptive Biosystems) using 485 nm excitation and 530 nm emission filter sets. The graph demonstrates the correlation between the fraction of LNCG-transduced cells and the fluorescence of each cell mixture (shown as an average of duplicate wells).

genes on such phenotypes as growth rate and cellular response to various treatments.

Quantitation of GFP Fluorescence with a Multiwell Fluorescence Reader. While most of our work relied on FACS for the detection of cells transduced with GFP retroviruses, we tested if the fluorescence of such cells would be high enough to be detected in living cells by a multiwell fluorescence reader. Different numbers of HT1080-3′SS6 cells transduced with LNCG virus and selected on G418 were added to non-infected cells to produce mixtures of various compositions. The graph in Fig. 4 demonstrates the correlation between the fraction of LNCG-transduced cells and fluorescence

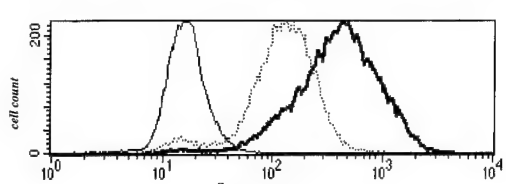

Fig. 5. Fluorescence profiles of HT1080-E14 populations infected at different concentrations of LRSN virus. HT1080-E14 cells were infected with LRSN virus from Bosc23 packaging cells with (dotted line) and without (solid line) 100-fold dilution of the viral stock. Following G418 selection, cells were analyzed by FACS using FACSort (Becton Dickinson) and compared with non-infected HT1080-E14 cells (fine line).

A

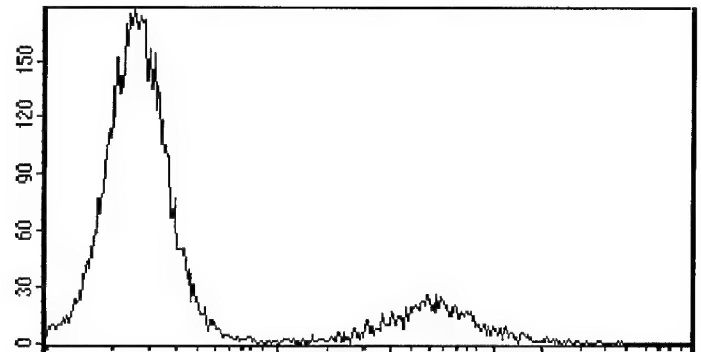

Initial representation	1.7%	10.6%	1%	0.2%
Average LXSE provirus number in single cell clones	1.0	1.0	1.3	2.0

B

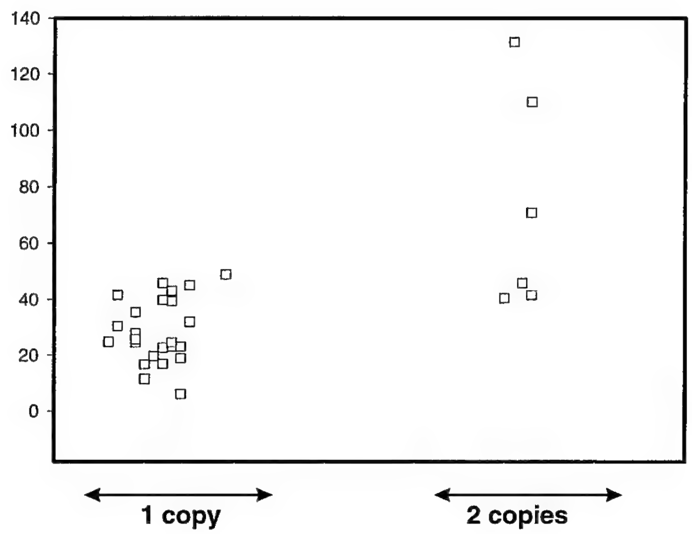

Fig. 6. Brighter LXSE infectants contain a higher number of integrated proviruses. Panel A. Fluorescence-based selection for higher-copy integrants. HT1080-3′SS6 cells were infected with LXSE virus from Bosc23 packaging cells. The histogram shows the fluorescence profile of the infected population. The four indicated positive areas were separated by flow sorting, and single-cell subclones were established from the sorted fractions. The copy number of integrated proviruses was estimated in individual subclones by Southern hybridization with an EGFP-specific probe. Panel B. Correlation between relative fluorescence and copy number of integrated proviruses in individual clones. Median fluorescence of individual clones, containing one or two copies of the integrated provirus was measured by flow cytometry and normalized for the medium fluorescence of uninfected cells.

of each cell mixture. The observed correlation is significant ($r^2 = 0.95$) and was reproduced in a number of similar experiments. The ability to detect and estimate the fraction of GFP-positive cells in a population using a multiwell fluorescence reader suggests that this simple procedure may be used to facilitate large-scale titration of recombinant retroviruses.

Fluorescence-Based Selection for Higher-Copy Integrants. We have previously observed

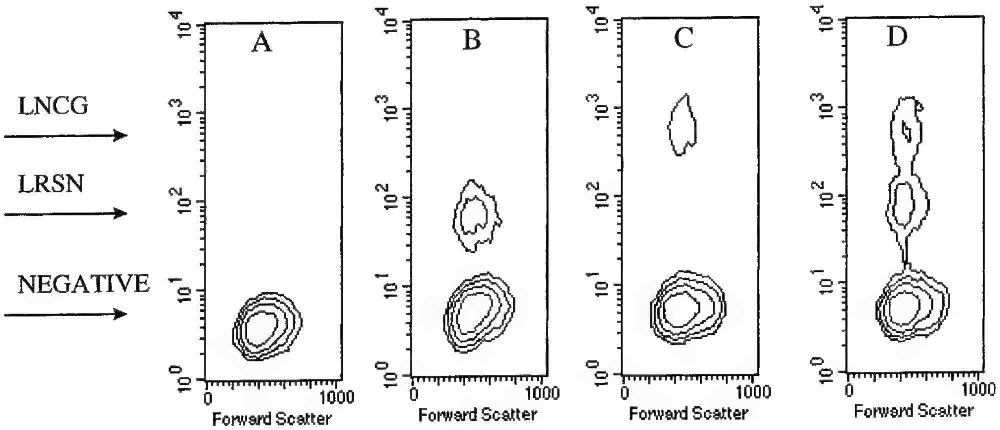

1ST INFECTION	MOCK	MOCK	LNCG	LRSN
2ND INFECTION	MOCK	LRSN	MOCK	LNCG

Fig. 7. Simultaneous detection of cells transduced with two different "red-shifted" GFP variants. HT1080-3′SS6 cells were mock-infected (panel A) or infected separately with LRSN or LNCG vectors (panels B and C) or consecutively with both vectors (panel D), and analyzed by FACS two days after the final infection. The results are presented as contour plots of fluorescence (Y axis) versus forward scatter (X axis) with one smoothing iteration and 3.2% threshold.

that cells transduced with retroviral vectors at different infection rates express the transduced genes at different levels, due to multicopy provirus integration at higher infection rates (1). To verify this observation using GFP vectors, HT1080-E14 cells were exposed to native and 100-fold diluted LRSN viral supernatant, yielding approximately 80% and 5% infection efficiencies, respectively. Upon completion of G418 selection, these two populations were compared by FACS (Fig. 5). The population initially transduced at a higher rate retained significantly higher median level of fluorescence, in agreement with the previous observations (1). This result underscores that a comparison of biological effects between different recombinant viruses should be performed at similar infection rates. It also indicates that comparison of GFP fluorescence in different constructs should be conducted at low infection rates, when the infectants are more likely to contain only a single copy of each provirus.

To isolate cells co-infected with different retroviruses or when higher expression of a retrovirally transduced gene is desired, it is advantageous to isolate a population of cells harboring more than one integrated provirus. We hypothesized that such a population may be obtained after infection with GFP vectors, through FACS selection of the brightest cells. We also expected that, unlike an increase in the stringency of drug selection (1), selection of brighter cells would not provide an opportunity for rare rearranged clones to overgrow the rest of the cells. To test these predictions we infected HT1080-3′SS6 cells with LXSE virus, with an infection rate of 13.5%. We then carried out FACS analysis on the infected population,

Fig. 8. Simultaneous detection of cells transduced with "red-shifted" and "blue-shifted" GFP variants. The results of FACS analysis carried out using Coulter Epics 753 flow cytometer are shown as density plots; X axis—green fluorescence, Y axis—blue fluorescence. Panel A. uninfected HT1080-3′SS6 cells. Panel B. HT1080-3′SS6 cells transduced with LNCB retrovirus and selected with G418. (Note a small but detectable fraction of EBFP-negative cells). Panel C. HT1080-3′SS6 cells, clone LXSE2-27 (a single-cell subclone of LXSE-transduced cells). Panel D. Cells of the clone LXSE2-27, superinfected with LNCB virus and selected with G418. Panel E. mixture of cells from B and C. Panel F. mixture of cells from A, B, C and D.

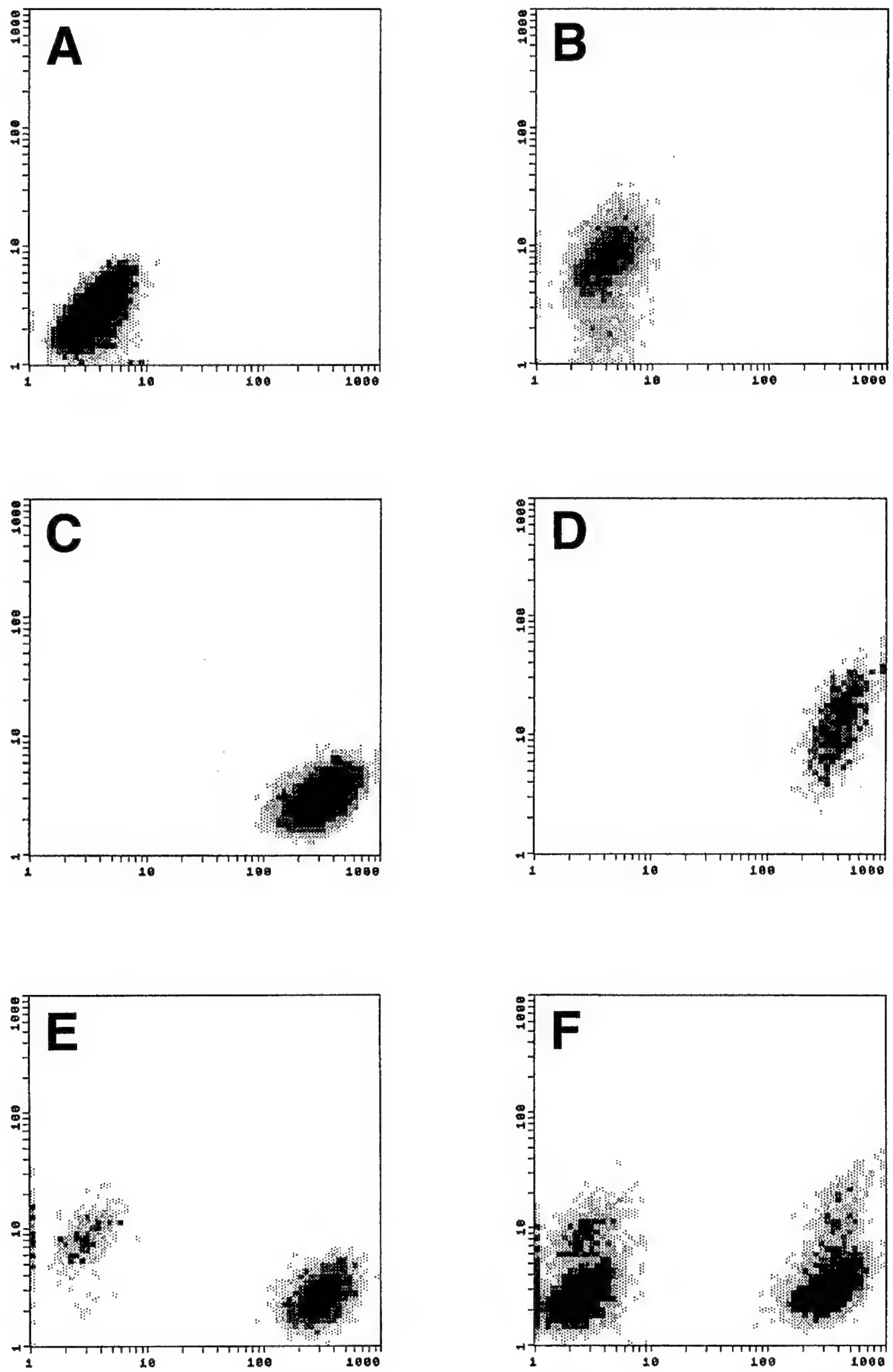

Fig. 8.

sorted out four different areas of the positive peak (Fig. 6A) and established a number of single-cell subclones from each of these areas. The copy number of integrated proviruses in each clone was estimated by Southern blotting and hybridization with an EGFP-specific probe. The average value obtained for each group of clones (3–12 clones in each group) is shown in Figure 6A. In agreement with our predictions, the brightest cells carried two proviruses, in contrast to the predominantly single-copy integrants in the rest of the positive peak (Fig. 6A and B), and no rearranged proviruses were detected in any of the clones by Southern hybridization (data not shown). Clones carrying either one or two copies of the provirus showed considerable variation in their relative fluorescence (Fig. 6B). This result emphasizes that comparison of gene expression by different vectors is more accurate if done on mass populations rather than individual clones of transduced cells.

Simultaneous Monitoring of Two Vectors Containing Different Forms of GFP. Many types of molecular genetic studies could benefit from the ability to monitor simultaneously two cell populations transduced with different genes. We have demonstrated the feasibility of using different forms of GFP as distinguishable fluorescent tags by simultaneous detection of two red-shifted variants of GFP characterized by different levels of cellular fluorescence. We have infected HT1080 cells with LRSN virus and then superinfected one half of these cells with LNCG. The superinfected cell population was compared by FACS to cells infected with LRSN alone, LNCG alone and the non-infected control. Figure 7 demonstrates that LRSN- and LNCG-infected cells form two distinct fluorescent populations. Although LNCG-infected and doubly-infected cell populations could not be distinguished from each other in the flow profiles, quantitative analysis of this experiment (not shown) revealed that LRSN-infected cells are efficiently superinfected with LNCG, since the fraction of the LRSN-positive population is reduced upon infection with LNCG.

An alternative approach to visualizing two different GFP-labeled cell groups at the same time is to use GFP forms with spectral properties that are sufficiently different to allow for independent observation. For this purpose, we constructed LNCB and LXSB vectors that contain the gene for BFP under the control of CMV promoter. Cells infected or transfected with these constructs were visualized as blue under fluorescent microscope equipped with a DAPI filter (data not shown). Also, cells expressing "blue", "red-shifted" or both GFP variants were distinguished from each other and from the non-infected cells by flow cytometry with simultaneous UV and blue excitation (Fig. 8). Besides obvious applications for simultaneous monitoring of cells infected with two different vectors, the availability of both EGFP and EBFP in similar vectors extends the opportunity for combination studies with other fluorophores. For example, EBFP (but not EGFP) can be used in combination with FITC, while EGFP (but not EBFP) can be used in combination with Hoechst dyes. In addition, both proteins can be combined with red dyes (such as propidium iodide) or orange dyes (such as phycoerythrine).

Use of GFP to Monitor the Expression of Promoters Transcribed in the Opposite Orientation. We have recently described inducible retroviral vectors that carry β-galactoside-regulated promoters, positioned in the opposite orientation to the LTR (15). When using such vectors, it is important to be able to monitor not only their presence in the cells but also the proper regulation of the inducible promoters. We hypothesized that in these constructs induction of an internal promoter would downregulate LTR-driven expression of a marker gene, due to antisense inhibition. Consequently, such changes in the expression of the marker might serve as an indicator for appropriate regulation of an inducible promoter.

To verify this prediction we have substituted *neo* with the "Green Lantern" GFP in three retroviral vectors carrying different β-galactoside-inducible promoters (15). The

resulting constructs (LGXRO2, LGXCO3 and LGXCO4; Fig. 1) were used to infect HT1080-3′SS6 cells that express LacI repressor modified for nuclear localization in mammalian cells. In the absence of inducers, the RF values of these vectors (Fig. 1) were inversely correlated to the previously characterized basal expression levels of the corresponding inducible promoters (15). To test if the induction of these promoters would decrease the GFP fluorescence, we infected HT1080-3′SS6 cells with LGXCO3 and selected GFP-positive cells. Upon short expansion, one half of the collected population was propagated in the presence and the other half in the absence of IPTG. Flow-cytometric comparison revealed a noticeable difference between induced and non-induced cells, with the induced cells showing greatly decreased fluorescence (Fig. 9). Subsequent return of the induced cells into IPTG-free medium brought their fluorescence to the level similar to that of the non-induced cells. As expected, changes in the fluorescence were inversely correlated with the changes in the expression from the internal modified CMV promoter, as measured by a RT-PCR assay (data not shown). Although several approaches exist to use GFP expression to monitor a regulated promoter (26), only in our system GFP fluorescence is detectable even when the gene of interest is not activated. Therefore, GFP can serve both as a marker and

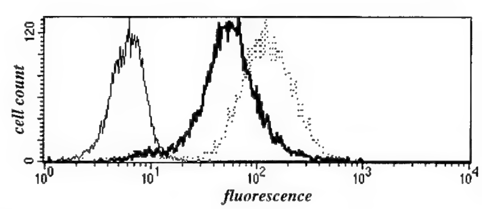

Fig. 9. Change of GFP expression in response to the activation of internal promoter in LGXCO3 vector. HT1080-3′SS6 cells were infected with LGXCO3 virus, GFP-positive subpopulation was collected and split into two parts. One part was cultivated in the presence, and the other in the absence of the inducer (5 mM IPTG). The histogram shows the fluorescence profiles of induced (solid line) and non-induced (dotted line) GFP-positive cells compared to the non-infected control (thin line). Induction of the modified CMV promoter was independently confirmed by RT-PCR (not shown).

as a reporter for delivery and expression of potentially cytotoxic or cytostatic genetic elements.

In conclusion, we have designed and characterized an extensive series of retroviral vectors that express different variants of GFP. These vectors provide a broad choice of promoter combinations, expression levels and detection options to be applicable to a diverse range of experimental protocols. These vectors are useful for gene delivery, tagging and tracking of specific cell groups within complex populations, optimization of transfection and transduction protocols, as well as for the studies of basic aspects of retroviral transduction. The use of GFP as a marker gene in retroviral constructs yields insights into structure-functional organization of retroviral vectors and extends the range of experimental goals achievable through retroviral transduction.

ACKNOWLEDGMENTS

We would like to thank Dr. K. Hagen, Dr. M. Polonskaia, and J. Altenhofen for assistance with flow cytometry, Dr. A. Neyfakh for help with fluorescent microscopy, Dr. E. Komarova for assistance with in vivo tumorigenesis assay, Dr. W.T. Beck for the use of a multiwell fluorescence reader, Drs. A.D. Miller, W. Pear, D. Baltimore, W. Chen and P. Chumakov for different plasmids and cell lines, and Drs. Y. Xuan and V. Levenson for helpful discussions. This work was supported by National Cancer Institute grants R01CA56736, R01CA62099 and R37CA40333 (I.B.R.), and grants DAMD17–94–J–4038 (I.B.R.) and DAMD17–96–1–6050 (E.S.K.) from the U.S. Army Medical Research and Materiel Command.

LITERATURE CITED

1. Schott, B., Iraj, E.S., and Roninson, I.B. (1996). Effects of infection rate and selection pressure on gene expression from an internal promoter of a double gene retroviral vector. *Somatic Cell Mol. Genet.* **22**:292–309.
2. Chalfie, M., Tu, Y., Euskirchen, G., Ward, W.W., and

Prasher, D.C. (1994). Green fluorescent protein as a marker for gene expression. *Science* **263:**802–805.
3. Delagrave, S., Hawtin, R.E., Silva, C.M., Yang, M.M., and Youvan, D.C. (1995). Red-shifted excitation mutants of the green fluorescent protein. *Bio/ Technology* **13:**151–154.
4. Heim, R., Cubitt, A.B., and Tsien, R.Y. (1995). Improved green fluorescence. *Nature* **375:**663–664.
5. Heim, R., Prasher, D.C., and Tsien, R.Y. (1994). Wavelength mutations and posttranslational autoxidation of green fluorescent protein. *Proc. Natl. Acad. Sci. U.S.A.* **91:**12501–12504.
6. Heim, R., and Tsien, R.Y. (1996). Engineering green fluorescent protein for improved brightness, longer wavelengths and fluorescence resonance energy transfer. *Curr. Biol.* **6:**178–182.
7. Mitra, R.D., Silva, C.M., and Youvan, D.C. (1996). Fluorescence resonance energy transfer between blue-emitting and red-shifted excitation derivatives of the green fluorescent protein. *Gene* **173:**13–17.
8. Anderson, M.T., Tjioe, I.M., Lorincz, M.C., Parks, D.R., Herzenberg, L.A., Nolan, G.P., and Herzenberg, L.A. (1996). Simultaneous fluorescence-activated cell sorter analysis of two distinct transcriptional elements within a single cell using engineered green fluorescent proteins. *Proc. Natl. Acad. Sci. U.S.A.* **93**(16):8508–8511.
9. Levy, J.P., Muldoon, R.R., Zolotukhin, S., and Link, C.J. Jr. (1996). Retroviral transfer of a humanized, red-shifted green fluorescent protein gene into human tumor cells. *Nature Biotechnology* **14:**606–609.
10. Muldoon, R.R., Levy, J.P., Kain, S.R., Kitts, P.A., and Link, C.J. Jr. (1997). Tracking and quantitation of retroviral-mediated transfer using a completely humanized, red-shifted green fluorescent protein gene. *Biotechniques* **22**(1):162–167.
11. Cheng, L., Fu, J., Tsukamoto, A., Hawley, R.G. (1996). Use of green fluorescent protein variants to monitor gene transfer and expression in mammalian cells. *Nature Biotechnol.* **14:**606–609.
12. Hanazono, Y., Yu, J.M., Dunbar, C.E., and Emmons, R.V. (1997). Green fluorescent protein in retroviral vectors: low titer and high recombination frequency suggest a selective disadvantage. *Hum. Gene Ther.* **8**(11):1313–1319.
13. Miller, D.A., and Rosman, G.J. (1989). Improved retroviral vectors for gene transfer and expression. *Biotechniques* **7:**980–986.
14. Morgenstern, J.P., and Land, H. (1990). Advanced mammalian gene transfer: high titer retroviral vectors with multiple drug selection markers and a complementary helper-free packaging cell line. *Nuc. Acid Res.* **18**(12):3587–3596.
15. Chang, B.-D., and Roninson, I.B. (1996). Inducible retroviral vectors regulated by lac repressor in mammalian cells. *Gene* **183:**137–142.
16. Grez, M., Zoring, M., Nowock, J., and Zeigler, M. (1991). A single point mutation activates the Moloney murine leukemia virus long terminal repeat in embryonal stem cells. *J. Virol.* **65**(9):4691–4698.
17. Pear, W.S., Nolan, G.P., Scott, M.L., Baltimore, D. (1993). Production of high-titer helper-free retroviruses by transient transfection. *Proc. Natl. Acad. Sci. U.S.A.* **90:**8392–8396.
18. Albritton, L.M., Tseng, L., Scadden, D., and Cunningham, J.M. (1989). A putative murine ecotropic retrovirus receptor gene encodes a multiple membrane-spanning protein and confers susceptibility to virus infection. *Cell* **57:**659–666.
19. Schott, B., Bennis, S., Pourquier, P., Ries, C., Londos-Gagliardi-D., and Robert, J. (1993). *Int. J. Cancer* **55:**115–121.
20. Zolotukhin, S., Potter, M., Hauswirth, W.W., Guy, J., and Muzyczka, N. (1996). A "humanized" green fluorescent protein cDNA adapted for high-level expression in mammalian cells. *J. Virol.* **70**(7):4646–4654.
21. Zhang, G., Gurtu, V., and Kain, S.R. (1996). An enhanced green fluorescent protein allows sensitive detection of gene transfer in mammalian cells. *Biochem. Biophys. Res. Commun.* **227:**707–711.
22. Cormack, B.P., Valdivia, R., and Falkow, S. (1995). FACS-optimized mutants of the green fluorescent protein (GFP). *Gene* **173:**33–38.
23. Bierhuizen, M.F., Westerman, Y., Visser, T.P., Wognum, A.W., and Wagemaker, G. (1997). Green fluorescent protein variants as markers of retroviral-mediated gene transfer in primary hematopoietic cells and cell lines. *Biochem. Biophys. Res. Commun.* **234**(2):371–375.
24. McBurney, M.W., Staines, W.A., Boekelheide, K., Parry, D., Jardine, K., and Pickavance, L. (1994). Murine PGK-1 promoter drives widespread but not uniform expression in transgenic mice. *Dev. Dyn.* **200**(4):278–293.
25. Ikawa, M., Kominami, K., Yoshimura, Y., Tanaka, K., Nishimune, Y., and Okabe, M. (1995). Green fluorescent protein as a marker in transgenic mice. *Devel. Growth Differ.* **37:**455–459.
26. Watsuji, T., Okamoto, Y., Emi, N., Katsuoka, Y., and Hagiwara, M. (1997). Controlled gene expression with a reverse tetracycline-regulated retroviral vector (RTRV) system. *Biochem. Biophys. Res. Commun.* **234**(3):769–773.

[CANCER RESEARCH 59, 3761–3767, August 1, 1999]

A Senescence-like Phenotype Distinguishes Tumor Cells That Undergo Terminal Proliferation Arrest after Exposure to Anticancer Agents[1]

Bey-Dih Chang, Eugenia V. Broude, Milos Dokmanovic, Hongming Zhu, Adam Ruth, Yongzhi Xuan, Eugene S. Kandel, Ekkehart Lausch, Konstantin Christov, and Igor B. Roninson[2]

Departments of Molecular Genetics [B-D. C., E. V. B., M. D., H. Z., A. R., Y. X., E. S. K., E. L., I. B. R.] and Surgical Oncology [K. C.], University of Illinois at Chicago, Chicago, Illinois 60607-7170

ABSTRACT

Exposure of human tumor cell lines to different chemotherapeutic drugs, ionizing radiation, and differentiating agents induced morphological, enzymatic, and ploidy changes resembling replicative senescence of normal cells. Moderate doses of doxorubicin induced this senescence-like phenotype (SLP) in 11 of 14 tested cell lines derived from different types of human solid tumors, including all of the lines with wild-type p53 and half of p53-mutated cell lines. SLP induction seemed to be independent from mitotic cell death, the other major effect of drug treatment. Among cells that survived drug exposure, SLP markers distinguished those cells that became terminally growth-arrested within a small number of cell divisions from the cells that recovered and resumed proliferation. SLP induction in breast carcinoma cells treated with retinoids *in vitro* or *in vivo* was found to correlate with permanent growth inhibition under the conditions of minimal cytotoxicity, suggesting that this response may be particularly important for the antiproliferative effect of differentiating agents. The senescence-like program of terminal proliferation arrest may provide an important determinant of treatment outcome and a target for augmentation in cancer therapy.

INTRODUCTION

Exposure of tumor cells to anticancer drugs leads to growth arrest and cell death. Drug-induced cell death often shows morphological and biochemical features of apoptosis (1, 2). Another form of cell death, induced by γ-irradiation (3) and some chemotherapeutic drugs (4–6), is termed mitotic cell death or mitotic catastrophe; it is characterized by the formation of micronuclei and accumulation of karyotypic abnormalities. Although mitotic death may culminate in features of apoptosis (7), only apoptosis and not mitotic death is promoted by wild-type p53 (8) and inhibited by BCL2 (5).

Induction of cell death is generally most prominent at the highest drug doses, whereas differentiating agents and low doses of chemotherapeutic drugs have a more pronounced cytostatic effect. Cellular damage by drugs or ionizing radiation induces transient growth arrest, which depends largely on the function of $p21^{waf1/cip1}$, a p53-regulated cyclin-dependent kinase inhibitor (9, 10). On removal of the drug, most tumor cells eventually resume division and either continue to proliferate or die with features of mitotic catastrophe (7, 11). Some of the drug-treated tumor cells undergo prolonged (up to several weeks) growth arrest; such stable arrest may show features of differentiation (12) and has been described as failure to resume cell division on release from the drug (9, 11).

In normal cells, terminal proliferation arrest may result from terminal differentiation or replicative senescence. Senescence, a physiological process that limits the proliferative span of normal cells, is accompanied by morphological changes (enlarged and flattened shape and increased granularity), shortening of telomeres, and accumulation of karyotypic abnormalities (13–15). A commonly used surrogate marker of senescence in human cells is the SA-β-gal[3] active at pH 6.0; this activity was shown to correlate with senescence in aging cell cultures *in vitro* and *in vivo* (16). Treatment of normal cells with DNA-damaging drugs or γ-irradiation (17–19) or introduction of an activated *ras* oncogene (20) rapidly induces terminal proliferation arrest accompanied by morphological features of senescence and the induction of SA-β-gal. Accelerated senescence was, therefore, suggested to be a programmed protective response of the organism to potentially carcinogenic impact (21). Like other damage responses of normal cells, such as quiescence and apoptosis (2, 22), senescence-like terminal proliferation arrest involves the function of wild-type p53 (18, 20, 23).

Escape from senescence in the course of neoplastic transformation has been linked to inactivation of p53 or $p16^{INK4a}$ (20, 24) and to constitutive activation of telomerase, an enzyme complex that prevents shortening of telomeres in consequent rounds of replication (25). Immortal tumor-derived cell lines, however, were reported to express senescence markers and to undergo terminal proliferation arrest after genetic modification, such as somatic cell fusion (26) or overexpression of *p53*, *RB*, *p16*, or *p21* tumor suppressor genes (27–30). Markers of senescence were also recently reported to develop in a nasopharyngeal carcinoma cell line after exposure to cisplatin, although the association of these markers with growth-restricted cells was not examined (31). These observations suggest that tumor cells have retained at least some of the components of the senescence-like program of terminal proliferation arrest. In the present study, we show that treatment of tumor cells with different classes of anticancer agents readily induces morphological, enzymatic, and ploidy changes characteristic of senescence, and that this SLP distinguishes cells that become stably growth-arrested within a small number of cell divisions from cells that recover after drug exposure. The induction of senescence-like terminal proliferation arrest may provide an important determinant of treatment response in tumor cells.

MATERIALS AND METHODS

Cell Lines. HT1080 subline 3′SS6 was derived in our laboratory (32). HCT116 cells were a gift from Dr. B. Vogelstein (Johns Hopkins University, Baltimore, MD). Most of the other cell lines were obtained from American Type Culture Collection. Cell lines DLD1, Saos2, LNCaP, and PC3 were grown in RPMI with 10% FC2 (Hyclone) or FCS; all of the other lines were grown in DMEM with 10% serum. Cell line MCF10AneoT, a gift from Dr. F. R. Miller (Karmanos Cancer Institute, Detroit, MI), was grown as a xenograft in nude mice by transplanting 2.2×10^6 cells mixed with 0.1 ml of Matrigel into the mammary gland parenchyma of both right and left inguinal glands of nude mice.

Received 1/29/99; accepted 5/21/99.

The costs of publication of this article were defrayed in part by the payment of page charges. This article must therefore be hereby marked *advertisement* in accordance with 18 U.S.C. Section 1734 solely to indicate this fact.

[1] Supported by National Cancer Institute Grants R01CA62099 and R37CA40333 (to I. B. R.) and predoctoral fellowship DAMD17-96-1-6050 from the United States Army Medical Research and Materiel Command (to E. S. K.).

[2] To whom requests for reprints should be addressed, at Department of Molecular Genetics (M/C 669), University of Illinois at Chicago, 900 South Ashland Avenue, Chicago, IL 60607-7170. Phone: (312) 996-3486; Fax: (312) 413-8358; E-mail: roninson@uic.edu.

[3] The abbreviations used are: SA-β-gal, senescence-associated β-galactosidase; 4-HPR, 4-hydroxyphenyl retinamide; FACS, fluorescence-activated cell sorter; FISH, fluorescence *in situ* hybridization; SLP, senescence-like phenotype; tRA, all-*trans*-retinoic acid; PI, propidium iodide.

Drug Assays, Microscopic Analyses, and FISH. All of the drugs were purchased from Sigma Chemical Co.; J. L. Shepherd Model 143 irradiator was used for γ-irradiation. Growth inhibition assays were carried out by plating 4–10 × 10^4 cells/3.5-cm plate before drug exposure; cell growth was measured by methylene blue staining, as described (33). Colony formation assays were done by plating 700 cells/10-cm plate and allowing cells to form colonies for 8 days after release from the drug. MCF10AneoT xenografts were allowed to reach 4–6 mm in diameter (4–5 weeks after injection), at which point the animals were separated into two groups, five animals with 10 tumors in each group. One group was left untreated, and the other group was given 4-HPR (4 mM/kg diet) for 2 months; the growth of tumor nodules was monitored.

Attached cells and frozen tumor sections were fixed and stained for SA-β-gal activity using X-gal (5-bromo-4-chloro-3-indolyl β-D-galactoside) at pH 6.0, as described (16); the percentage of SA-β-gal+ cells was determined by bright-field microscopy after scoring 100-1000 cells for each sample. Micronuclei formation was determined after SA-β-gal staining, either by phase-contrast microscopy or after staining with H&E. [^{3}H]thymidine autoradiography was carried out as described (16).

FISH analysis of interphase nuclei was conducted by the Reproductive Genetics Institute (Chicago, IL) using mixtures of differentially labeled fluorescent probes specific for human chromosomes 18 and 21 or 13, 18, 21, X, and Y, using the hybridization conditions and scoring criteria recommended by the probe manufacturer (Vysis, Downers Grove, IL). Fluorescent cells were examined and photographed using Nicon fluorescence microscope with Photometrics Sensys camera and Quips mFISH imaging software.

FACS Assays. For DNA content analysis, 3 × 10^5 cells/6-cm plate were treated with different drugs. After treatment, floating cells were collected by centrifugation, combined with trypsinized attached cells, and analyzed by PI staining and FACS analysis using Becton Dickinson FACSort, as described (34).

For PKH2 analysis of cell division, 10^7 cells were trypsinized and labeled with PKH2 (Sigma Chemical Co.), according to the manufacturer's protocol. Cells were plated at 2 × 10^5/6-cm plate, and PKH2 fluorescence was monitored on consecutive days by FACS analysis, after PI staining to exclude dead cells. As a control for the stability of PKH2 labeling, no changes in cell fluorescence were observed in a HT1080 subline that was growth-arrested for 5 days by inducible overexpression of p21$^{waf1/cip1}$. ModFit cell cycle analysis program (Verity Software) was used to determine the percentage of cells that went through different numbers of divisions. Cell sorting was carried out using FACSvantage (Becton Dickinson) or EPICS Elite-ESP (Coulter). The sorted cells were used for SA-β-gal staining after plating 5 × 10^4 cells/3-cm plate and for clonogenic assays by plating 2000 cells/10-cm plate.

RESULTS

Moderate Doses of Cytotoxic Agents Induce Mitotic Cell Death and SLP. We have analyzed the effects of a moderate (30 nM) dose of doxorubicin, a widely used anticancer agent that acts by stabilizing "cleavable complexes" of DNA with topoisomerase II, on HT1080 human fibrosarcoma cells. This cell line carries mutant N-*ras* (35), is p16-deficient (24), and expresses wild-type Rb (36) and p53.[4] As illustrated in Fig. 1*A*, doxorubicin treatment produced a mixed cytostatic and cytotoxic effect, evidenced by pronounced growth arrest by the 2nd day of exposure and a decrease in cell number detectable from the 3rd day. The most prominent feature of cell death was the appearance of enlarged cells containing multiple completely or partially separated micronuclei with evenly stained chromatin (Fig. 2*A*). FISH with chromosome-specific probes indicated that fragmented nuclei contained an increased number of chromosomes, which were unevenly distributed among the micronuclei (Fig. 2*B*). Such nuclear changes are characteristic of mitotic catastrophe (5, 6). The percentage of attached micronucleated cells increased over the time of exposure (Fig. 1*B*). As previously reported for γ-irradiated HT1080 cells (37), doxorubicin treatment produced little evidence of apoptosis, judging by the rarity of cells with apoptotic morphology, terminal deoxynucleotidyl transferase-mediated nick end labeling-positive cells, or cells with elevated annexin levels (data not shown). The only measurable change that is usually associated with apoptosis (but may also reflect the formation of micronuclei; Ref. 6) is the appearance of nuclei with decreased (sub-G_1) DNA content, detected after combining attached and floating cells on each plate (Fig. 1*B*). The removal of drug after 3 days slightly accelerated the process of cell death (Fig. 1*A*) and increased the percentages of micronucleated and sub-G_1 cells (Fig. 1*B*).

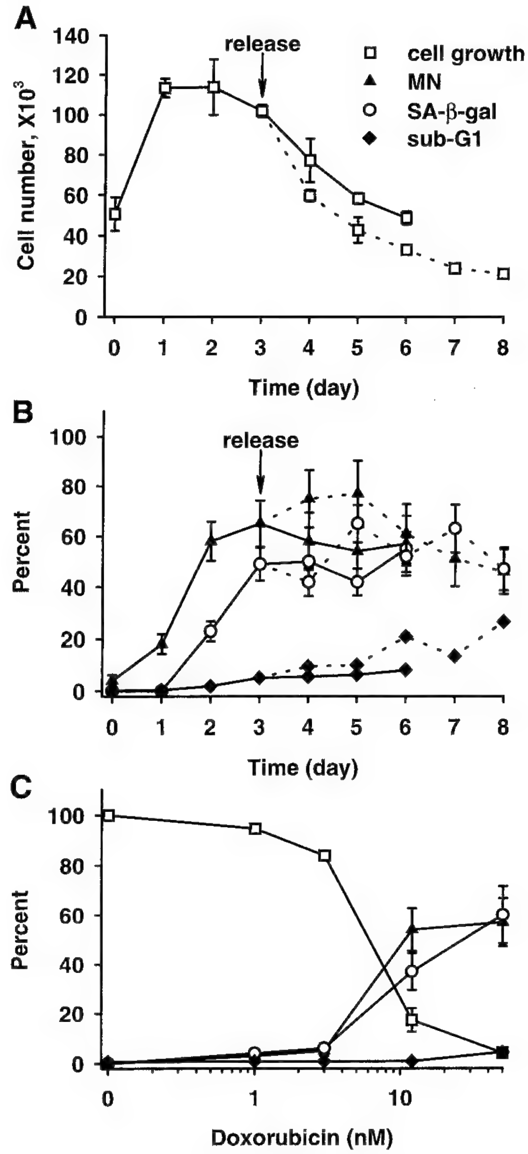

Fig. 1. Effects of doxorubicin on HT1080 3′SS6 cells. *A*, changes in cell number during treatment with 30 nM doxorubicin. Cells were exposed to drug either continuously (*solid lines*) or released from the drug after 3 days of exposure (*dashed lines*). *B*, changes in the percentages of cells with multiple micronuclei (*MN*), SA-β-gal+ cells, and cells with sub-G_1 DNA content during treatment with 30 nM doxorubicin. *Bars*, the Poisson SD calculated as the square root of counted events and expressed as percentages. *C*, growth inhibition (cell number relative to untreated cells) and percentages of cells with multiple micronuclei, SA-β-gal+ cells and cells with sub-G_1 DNA contents, as a function of doxorubicin concentration on 4-day exposure.

Many doxorubicin-treated cells also showed phenotypic changes that resembled features of senescence in normal fibroblasts. This SLP included enlarged and flattened morphology, expression of the senescence marker SA-β-gal detectable by 5-bromo-4-chloro-3-indolyl β-D-galactoside (X-gal) staining at pH 6.0 (Fig. 2c,d) and increased granularity (see below). SA-β-gal expression was observed in only

[4] B. Schott and I. B. Roninson, unpublished data.

Fig. 2. Formation of micronuclei and SA-β-gal expression in drug-treated cells. Attached cells (*A* and *C-H*) or frozen sections (*I* and *J*) were fixed with 2% formaldehyde/0.2% glutaraldehyde and stained for SA-β-gal activity; cells were counterstained with H&E (*A*) and autoradiographed (*E*). The photographs were taken at 400-fold (*A*; 20-μm scale bar), 1000-fold (*B*), 200-fold (*C-H*; 50-μm scale bar in *C*), or 400-fold (*I* and *J*; 30-μm scale bar in *I*) magnification. *A*, multiple micronuclei in HT1080 (3'SS6) cells treated with 30 nM doxorubicin for 3 days. *B*, FISH analysis of chromosome distribution among the micronuclei in a partially fragmented nucleus of HT1080 cells treated with 20 nM doxorubicin for 3 days. Cells were hybridized with a mixture of fluorescent probes specific for chromosomes 18 (*green*) and 21 (*red*); nuclei were stained with DAPI (*blue*). *C*, untreated HT1080 cells. *D*, HT1080 3'SS6 cells exposed to 30 nM doxorubicin for 4 days. *E*, HT1080 3'SS6 cells treated with 20 nM doxorubicin for 3 days and grown without drug for 4 days, with [^{3}H]thymidine added for the last 2 days. *F*, untreated MCF-7 cells. *G*, MCF-7 cells exposed to 50 nM doxorubicin for 2 days. *H*, MCF-7 cells exposed to 100 nM tRA for 8 days. *I*, xenograft tumor formed by MCF10AneoT cells in nude mice, untreated. *J*, MCF10AneoT xenograft treated *in vivo* with 4-HPR.

1–3% of untreated subconfluent cells, but this percentage rose sharply after 2 days of drug exposure and reached 55% by day 6 (Fig. 1*B*). The removal of doxorubicin on day 3 had no significant effect on the SA-β-gal+ fraction (Fig. 1*B*). On 4-day exposure to different doses of doxorubicin, the percentages of micronucleated and SA-β-gal+ cells showed similar magnitude and drug dose dependence, whereas the sub-G_1 fraction remained low (Fig. 1*C*). The intensity of cellular staining for SA-β-gal also increased in a time- and dose-dependent manner (data not shown). SA-β-gal+ and SA-β-gal− cells underwent mitotic death with a similar probability. For example, cell population treated with 30 nM doxorubicin for 3 days showed micronucleation in 70 ± 8.1% of SA-β-gal+ and 67 ± 8.6% of SA-β-gal− cells; analysis of two other drug-treated populations also showed no significant differences in micronucleation between SA-β-gal+ and SA-β-gal− cells, suggesting that the induction of SLP and mitotic cell death were independent events.

We have also analyzed the response of HT1080 3'SS6 cells to other cytotoxic drugs or ionizing radiation at doses that induced 85% growth inhibition after 4-day continuous exposure (ID_{85}). As summarized in Table 1, all of the agents induced micronucleation in a large fraction (45–66%) of treated cells, whereas the sub-G_1 fraction did not exceed 13% for any of the tested drugs. The increase in the percentage of SA-β-gal+ cells varied for different agents, with the strongest effect (>50%) observed with doxorubicin, aphidicolin, and cisplatin and the weakest effect (<10%) observed with microtubule-affecting agents vincristine and Taxol (Table 1). Induction of reversible growth arrest by serum withdrawal produced faint SA-β-gal staining in some of the cells, but the staining intensity was weaker than in cells treated with any of the drugs. Thus, induction of SLP and mitotic death seem to be common responses of HT1080 cells to different classes of drugs.

SLP Is Associated with Restricted Proliferative Capacity. To investigate whether drug-induced SLP is associated with a restricted proliferative capacity, as would be expected for senescent cells, HT1080 cells were treated with 20 nM doxorubicin for 3 days and then labeled with a lipophilic fluorescent compound, PKH2. PKH2 incorporates stably into plasma membrane and is evenly divided between daughter cells, allowing one to distinguish cells that underwent a different number of divisions by their decreasing PKH2 fluorescence (38). FACS analysis of cells released into drug-free media (Fig. 3*A*) showed that drug-treated cells started dividing on the 1st day after release from the drug, but they divided slower and more heterogeneously than the untreated cells. By day 5 after release from the drug, a shoulder of growth-retarded cells became distinct from the peak of proliferating cells, and PKH2 fluorescence of this shoulder remained almost unchanged on subsequent days (Fig. 3*A*). By day 6, the proliferating cells went through four to five cell divisions, whereas 84% of growth-retarded cells divided only once or twice. Only 8–14% of the growth-retarded cells failed to divide at least once after release from the drug, indicating that growth retardation in this population was not merely a failure to reenter cell cycle after drug-induced growth arrest.

To investigate the association between growth retardation, SLP, and clonogenic potential of drug-treated cells, we have used FACS analysis to separate the growth-retarded and proliferating fractions after drug treatment. We have observed that growth-retarded cells with high PKH2 fluorescence also showed elevated 90-degree light scatter [side scatter (*SS*)] relative to untreated cells (Fig. 3*B*). Elevated side scatter is characteristic of senescent cells and may reflect increased cell size (39) and number of lipofuscin granules (27). Fractions enriched in growth-retarded ($PKH2^{hi}$ SS^{hi}) or proliferating

Table 1 *Effects of different agents on HT1080 3'SS6 cells*

Agent	ID_{85}	% SA-β-gal+	% micronucleated	% sub-G_1
None		1	1.5	0.4
Doxorubicin	30 nM	79	45	10
Aphidicolin	200 ng/ml	64	45	10
Cisplatin	2.2 μM	55	47	9.3
γ-irradiation	1300 rad	36	63	3.2
Cytarabine	1.5 μM	23	64	7.5
Etoposide	900 nM	15	55	7.5
Taxol	5 ng/ml	9.1	66	7.1
Vincristine	1.5 nM	3.1	62	13

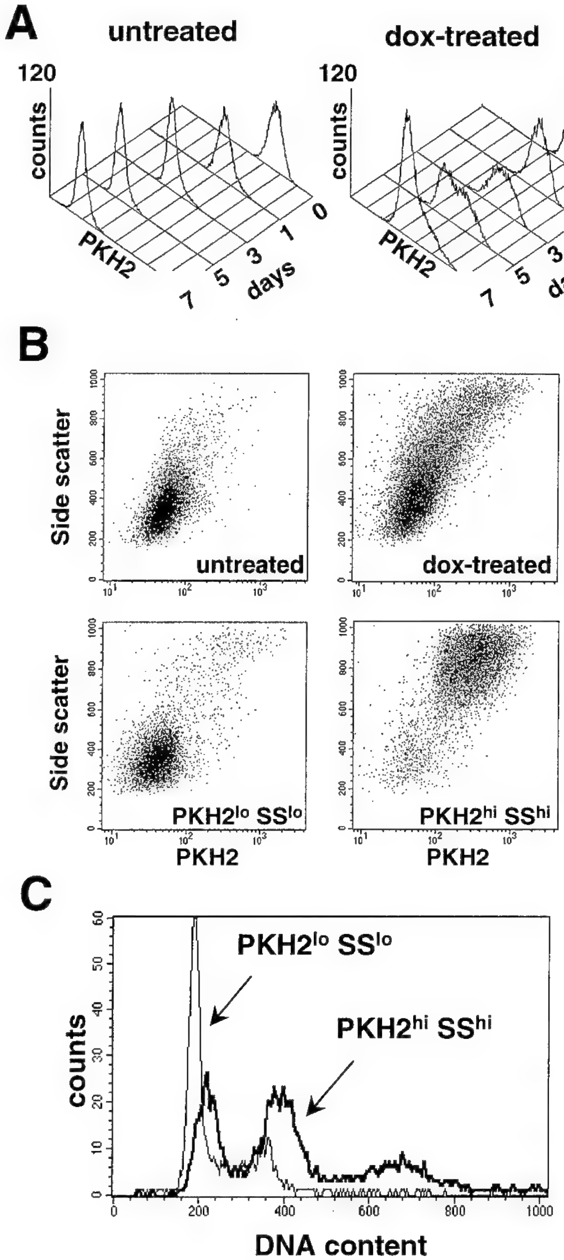

Fig. 3. Flow cytometric analysis of PKH2-labeled HT1080 3′SS6 cells. *A*, changes in PKH2 fluorescence profiles in untreated cells (*left*) and in cells exposed to 20 nM doxorubicin for 3 days, labeled with PKH2, and plated in drug-free medium (*right*). Cells were analyzed by FACS analysis on consecutive days after release from the drug (day 0). For untreated cells, 10,000 PI-negative cells were analyzed on each day. For drug-treated cells, each profile corresponds to the same number of initially plated cells to reflect changes in the cell number. *B*, increased side scatter in growth-retarded cells. Dot density maps of PKH2 fluorescence (*X* axis) and 90-degree light scatter (*Y* axis) are shown for PKH2-labeled untreated cells (*top left*); cells treated for 3 days with 20 nM doxorubicin, labeled with PKH2, and grown without drug for 6 days (*top right*); and for PKH2^{lo} SS^{lo} (*bottom left*) and PKH2^{hi} SS^{hi} (*bottom right*) fractions isolated from the above population by FACS. *C*, DNA content analysis of PKH2^{lo} SS^{lo} (99% pure) and PKH2^{hi} SS^{hi} (95% pure) cell populations isolated by two rounds of FACS sorting after 3 day exposure to 20 nM doxorubicin and 5-day growth without drug.

(PKH2^{lo} SS^{lo}) cells were sorted out 5 or 6 days after release from the drug (Fig. 3*B*). The sorted populations were then analyzed for SA-β-gal activity, clonogenicity, and DNA content. The results of three independent sortings are summarized in Table 2. SA-β-gal expression was associated with the growth-retarded fractions, and the percentage of SA-β-gal+ cells in each fraction was close to the percentage of PKH2^{hi} SS^{hi} cells. Colony formation assays showed that PKH2^{hi} SS^{hi} fractions had greatly decreased colony-forming ability relative to PKH2^{lo} SS^{lo} fractions. The residual clonogenicity of growth-retarded fractions correlated with the percentage of PKH2^{lo} SS^{lo} or SA-β-gal− cells in such fractions and was most probably attributable to contamination with proliferating cells (Table 2). Thus, SLP distinguishes cells with restricted proliferative capacity from cells that continue proliferation after release from the drug.

The decreased growth and restricted proliferative capacity of SLP cells were confirmed by other types of assays. For example, we have used [^{3}H]thymidine autoradiography to identify cells that replicated their DNA over a 48-h period starting 3 or 4 days after release from 20 nM doxorubicin (Fig. 2*E*). In two independent experiments, 92–93% of SA-β-gal− cells incorporated [^{3}H]thymidine, but only 28–33% of the SA-β-gal+ population became labeled, indicating that fewer SA-β-gal+ cells underwent DNA replication in the last 2 days before staining. We have also analyzed the long-term proliferation of a largely SLP cell population that survived exposure to a higher drug dose. 10^5 cells were treated with 60 nM doxorubicin for 3 days. Seven days after release from the drug, 15,000 cells remained attached to the plate. Ninety-eight percent of these cells were SA-β-gal+, and ~50% contained micronuclei. Most of these cells eventually died and detached from the plate, but about 1500 SA-β-gal+ single cells or small clusters (<10 cells) remained attached 24 days after release from the drug. Despite periodic renewal of the media, only 25 cell colonies (all SA-β-gal−) grew out by the end of the experiment, indicating that most, if not all, SLP cells lost their long-term proliferative capacity.

Ploidy Changes in SLP Cells. FACS analysis was used to determine the DNA content of PKH2^{lo} SS^{lo} and PKH2^{hi} SS^{hi} fractions isolated 5 days after release from doxorubicin. As shown in Fig. 3*C*, the proliferating (PKH2^{lo} SS^{lo}) fraction showed cell cycle distribution characteristic for exponentially growing cells (high G_1 and S). The growth-retarded (PKH2^{hi} SS^{hi}) fraction showed a heterogeneous DNA content, with broader G_1 and G_2 peaks than in proliferating cells and a substantial fraction of cells with higher than G_2 DNA content. FISH analysis of interphase nuclei confirmed ploidy changes in the growth-retarded cells. Most of the untreated cells were trisomic or near trisomic for chromosomes 13, 18, 21, and X/Y, indicating that the HT1080 3′SS6 line was near-triploid. In contrast, approximately one-half of the cells in the growth-retarded fraction contained enlarged nuclei with four copies of each of the autosomes, whereas ~20% had six or more copies (data not shown). Increased DNA ploidy has been previously associated with terminal stages of senescence in normal fibroblasts (13).

Responses to Doxorubicin in Different Tumor Cell Lines. We have examined cellular changes induced by treatment with moderate doses of doxorubicin in other solid tumor-derived human cell lines. Fourteen lines derived from 10 different types of cancer were treated for 2 days with the doses of doxorubicin that induced 70–90% growth inhibition. The effects of this treatment on the formation of micronuclei, sub-G_1 fraction, and the SA-β-gal+ phenotype are summarized

Table 2 *Analysis of sorted populations of growth-retarded and proliferating fractions of doxorubicin-treated HT1080 cells*[a]

Experiment	Fraction	% PKH2^{hi} SS^{hi}	% SA-β-gal+	No. of colonies/1000 cells
1	GR[b]	82%	64%	26
	P	7%	4.8%	210
2	GR	75%	53%	62
	P	1%	1.2%	254
3	GR	80%	76%	11
	P	1%	3.7%	93

[a] HT1080 (3′SS6) cells were treated with 20 nM doxorubicin for 3 days, labeled with PKH2, and grown without drug for 5 days (experiment 3) or 6 days (experiments 1 and 2).

[b] Growth-retarded (GR) and proliferating (P) cells were isolated by FACS.

Table 3 *Effects of 2-day treatment with moderate doses of doxorubicin in cell lines derived from different types of human solid tumors*

Cell line	Tumor type	Doxorubicin concentration	p53 status[a]	Increased SA-β-gal[b]	Increased micronuclei formation[c]	Increased sub-G_1[d]
HT1080	Fibrosarcoma	20–30 nM	wt[e]	+	+	+
HCT116	Colon carcinoma	50 nM	wt	+	+	++
MCF-7	Breast carcinoma	12–50 nM	wt	+[f]	++	−
HepG2	Hepatocellular carcinoma	250–500 nM	wt	+	++	++
A2780	Ovarian carcinoma	20–50 nM	wt	+[f]	A	+++
LNCaP	Prostate carcinoma	100–500 nM	wt	+[f]	A	+++
HeLa	Cervical carcinoma	400–800 nM	wt/E6	+	++	+
HEp-2	Larynx carcinoma	50–100 nM	wt/E6	+[f]	+	−
DLD1	Colon carcinoma	100–500 nM	mt (241)	−	+	+
SW480	Colon carcinoma	100–150 nM	mt (273)	+	+	−
U251	Glioma	200 nM	mt (273)	+	++	−
MDA-MB-231	Breast carcinoma	50 nM	mt (280)	−	++	−
PC3	Prostate carcinoma	100 nM	mt (del138)	−	+++	++
Saos2[g]	Osteosarcoma	50–60 nM	mt (del)	+	+	++

[a] p53 status of the listed cell lines is from Refs. 48–55.
[b] Positive (*) indicates ≥3-fold increase in the percentage of SA-β-gal+ cells.
[c] Micronucleated cells: +, 20–50%; ++, 50–80%; +++, ≥80%; A, predominance of cells with apoptotic morphology.
[d] Sub-G_1 cells: +, 5–10%; ++, 10–30%; +++, ≥30%.
[e] Wt, wild type; mt, mutant.
[f] More than 10% SA-β-gal+ cells without drug treatment.
[g] Because of long doubling time of Saos2 cells, all the assays were carried out after 4-day exposure to doxorubicin.

in Table 3. Drug treatment increased the fraction of micronucleated cells in almost all of the cell lines, but only two lines (LNCaP and A2780) showed predominant morphological changes characteristic of apoptosis. The same two lines were the only ones to develop a very high (≥48%) sub-G_1 fraction (Table 3), suggesting that mitotic death may be more common than apoptosis among solid tumor cell lines exposed to moderate doses of doxorubicin.

SA-β-gal+ cells with morphological features of senescence were induced by doxorubicin treatment in 11 of 14 lines (Table 3). One of these lines, HCT116 colon carcinoma was analyzed with regard to a correlation between SA-β-gal staining and growth arrest. HCT116 cells were treated with 50 nM doxorubicin for 3 days and stained for SA-β-gal expression 10–11 days after release from the drug. At this point, the proliferating cell colonies were almost entirely SA-β-gal−, whereas attached single cells were mostly SA-β-gal+, indicating that SA-β-gal expression in this cell line was associated primarily with cells that failed to divide even once after release from the drug.

SA-β-gal induction was observed in all eight of the tested lines that carry wild-type p53, including two lines in which the function of p53 is inhibited by the E6 papilloma virus protein. Several cell lines (MCF-7, A2780, LNCaP, and HEp-2) showed noticeable SA-β-gal positivity (>10%) even without drug treatment, but these levels were further increased on exposure to doxorubicin (as illustrated for MCF-7 cells in Fig. 2, *F* and *G*). SA-β-gal expression of untreated cells varied depending on the media and among subclones; it remains to be determined whether the background SA-β-gal activity marks cells that spontaneously lose their proliferative capacity. Doxorubicin also induced SA-β-gal in three of six p53-mutant cell lines, including Saos-2, which is deficient not only for p53 but also for Rb. All three lines that failed to show SA-β-gal induction under the tested conditions were p53-mutant. Thus, induction of the SA-β-gal marker of senescence by drug treatment is common in solid tumor cells and may partly correlate with the p53 status.

Cytostatic Treatment with Retinoids Induces SLP in Breast Carcinoma Cells *in Vitro* and *in Vivo*. Inhibition of tumor cell growth by doxorubicin and other chemotherapeutic drugs depends both on their cytotoxic and cytostatic effects. To determine whether SLP would be induced by agents, the action of which is primarily cytostatic, we have investigated the effect of retinoids that cause differentiation-associated permanent growth arrest in breast carcinoma cells (40). MCF-7 breast carcinoma cells were labeled with PKH2 and grown in the presence or absence of 100 nM tRA. FACS analysis of PKH2 fluorescence indicated that tRA-treated and untreated cells divided at the same rate over the first 4 days, but retinoid-treated cells slowed down their division by day 6, and essentially stopped dividing between days 6 and 9 (Fig. 4*A*). Concurrent determination of the cell number showed that tRA-treated cells started growing slower than untreated cells between days 4 and 6, and showed only a small (20%) decrease in cell number between days 6 and 9 (Fig. 4*B*). These results, together with a small difference in the number of dead (propidium iodide-positive) cells between tRA-treated and untreated samples, indicated that growth inhibition of

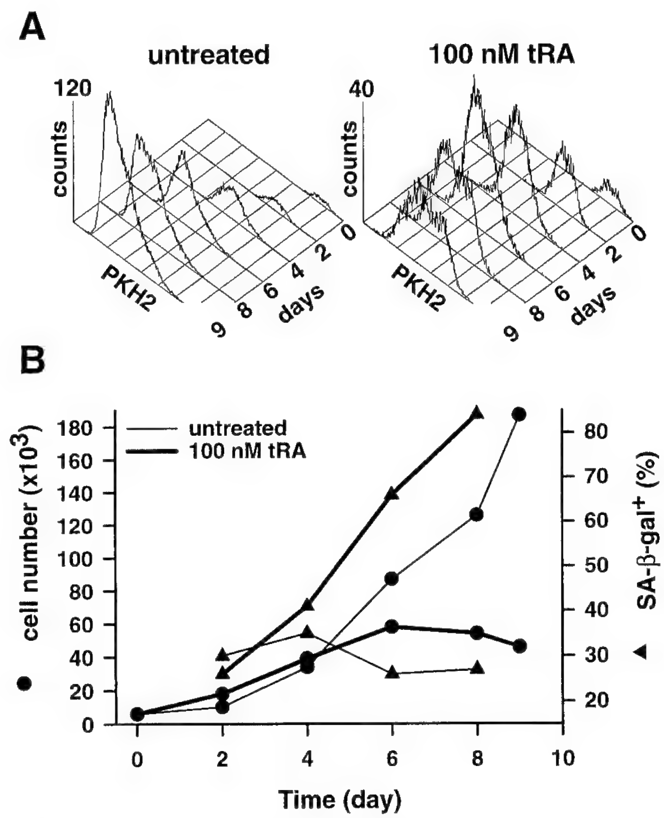

Fig. 4. Effects of tRA on MCF-7 cells *A*, PKH2 profiles of untreated MCF-7 cells and cells treated with 100 nM tRA for the indicated number of days. Each profile corresponds to the same number of initially plated cells. *B*, time course of changes in cell number (●) and percentages of SA-β-gal+ cells (▲) for MCF-7 cells, untreated or treated with 100 nM tRA.

MCF-7 cells by 100 nM tRA was due primarily to the cytostatic effect of this agent. The clonogenicity of cells treated for 9 days with tRA decreased >100-fold relative to untreated cells, indicating permanent nature of this cytostatic growth inhibition.

Retinoid-treated MCF-7 cells showed enlarged and flattened morphology and increased granularity. These changes have been described as characteristic of differentiation in this cell line (12, 41), but can also be viewed as indicative of a senescence-like process. In agreement with this interpretation, tRA treatment drastically increased SA-β-gal expression in MCF-7 cells (Fig. 3, *F* and *H*). The percentage of SA-β-gal+ cells increased in parallel with growth inhibition and reached 84% on day 8 (Fig. 4*B*). Thus, the induction of SLP correlates with retinoid-induced cytostatic growth arrest.

We have also investigated whether SLP could be induced by retinoid treatment *in vivo*. As a model system, we have used H-*ras*-transformed MCF10ANeoT human breast epithelial cell line; when grown as a xenograft in athymic nude mice, this line forms hyperplastic and premalignant lesions with characteristics of ductal hyperplasia and carcinoma *in situ* of human breast (42). Previous *in vitro* studies indicated that 4-HPR, an inhibitor of mammary carcinogenesis, suppresses cell proliferation in MCF10AneoT cells (43). MCF10AneoT cells were transplanted into the mammary gland parenchyma of both inguinal glands of 10 nude mice. After 4–5 weeks, 4–6 mm/diameter tumor nodules occurred in all animals. Two groups, each including five animals (10 tumors), were either untreated or treated with 4-HPR for 2 months at 4 mM/kg diet. Untreated tumors showed three types of glandular structures: simple tubular (20%), hyperplastic tubular (58%), and premalignant with dysplastic epithelial cells (22%). 4-HPR-treated tumors showed an increase in simple tubular structures (55%) and a decrease in tubular hyperplastic (35%) and premalignant structures (10%). These observations suggested that 4-HPR induced differentiation in MCF10ANeoT xenografts. Frozen sections from 4-HPR-treated and untreated tumors were stained for SA-β-gal expression. Both tumors showed detectable SA-β-gal staining in xenograft epithelial cells. In the untreated tumor, the staining was of low intensity and localized to limited tumor areas (Fig. 2*I*), whereas the drug-treated tumor showed higher SA-β-gal staining intensity with relatively uniform distribution among the tumor cells (Fig. 2*J*), suggesting that retinoid treatment *in vivo* induced SLP in tumor cells.

DISCUSSION

Induction of accelerated senescence was proposed to be a programmed protective response of normal cells to potentially carcinogenic impact (21). In this regard, rapid senescence serves a similar function to apoptosis; remarkably, both of these responses to cellular damage are regulated largely by p53. It is well appreciated that the program of apoptosis is retained in many types of leukemias and solid tumors, and that apoptosis contributes to tumor response to anticancer agents. Senescence, however, has been viewed primarily as a property of normal cells, which is lost during neoplastic transformation. The results of the present study indicate that phenotypic and proliferative changes that resemble terminal stages of replicative senescence can be induced in tumor cells not only through genetic modifications but also epigenetically, by treatment with different classes of anticancer agents. Drug-induced SLP distinguishes cells with restricted proliferative potential from those that continue to proliferate after drug exposure, suggesting that senescence-like terminal proliferation arrest is an important determinant of treatment response in human cancer.

Cellular changes that define SLP include enlarged and flattened morphology, increased granularity, expression of SA-β-gal, and ploidy changes. All of these features have been originally associated with terminal stages of replicative senescence in normal fibroblasts (13, 16). There are some obvious differences, however, between the slow process of replicative senescence (about 50 cell doublings) and the more rapid forms of terminal proliferation arrest, activated in normal or tumor cells in response to different stimuli. Most significantly, replicative senescence is mediated, at least in part, by the shortening of telomeres (25), but there is no apparent decrease in telomerase activity in drug-treated HT1080 cells (44), in nasopharyngeal carcinoma cells that display SLP after cisplatin treatment (31), or in tumor cells that are growth-arrested by overexpression of p53 (28). Telomere shortening during senescence was suggested to trigger terminal proliferation arrest through p53 activation (45). p53 also plays a key role in senescence-like terminal proliferation arrest induced by DNA damage or *ras* mutation in normal cells (18, 20). In the present study, all three cell lines that failed to induce SLP after treatment with moderate doses of doxorubicin were p53-deficient, whereas this response was observed in all cell lines with wild-type p53. As will be reported elsewhere (46), p53 acts as a positive regulator of drug-induced SLP in HT1080 and HCT116 cell lines, although its function is not absolutely required for this drug response. These observations suggest that various physiological and damage-induced stimuli may activate the same senescence-like response in normal and tumor cells and that SLP marks this common program of terminal proliferation arrest.

In cells treated with cytotoxic drugs, SLP induction and cell death seem to be concurrent and independent responses. Thus, SA-β-gal+ and SA-β-gal− cells have a similar probability of undergoing mitotic death during drug treatment or on the first few days after release from the drug. Once the rapid process of cell death is completed, however, SLP distinguishes the subpopulation of growth-retarded and nonclonogenic cells from the cells that recover and proliferate normally. The overall outcome of treatment with chemotherapeutic drugs is, therefore, determined by the combination of factors responsible for the induction of cell death (mitotic death or apoptosis) and senescence-like terminal proliferation arrest. Exposure to moderate doses of doxorubicin induced SLP in 11 of 14 tested cell lines derived from different types of human solid tumors. Among the different effects of doxorubicin in this panel of tumor cell lines, mitotic cell death and SLP seem to be more common than apoptosis. SLP is relatively more prominent at less cytotoxic drug doses (such as 20–100 nM doxorubicin), which can be readily induced and maintained for a long period of time in patients' plasma by continuous infusion (47). Senescence-like terminal proliferation arrest may, therefore, be a significant determinant of tumor response to continuous infusion protocols. On the other hand, SLP correlates with permanent growth inhibition of breast carcinoma cells by retinoids, under the conditions in which the induction of cell death plays a minimal role in their antiproliferative effect. Thus, SLP induction may be the primary determinant of treatment outcome for cytostatic differentiating agents.

Analysis of SLP markers in clinical cancer may provide an important diagnostic approach to monitoring tumor response to different forms of therapy. SA-β-gal expression is thus far the only quantifiable marker associated with drug-induced SLP *in vitro* and *in vivo*. In the present study, drug-induced SA-β-gal expression was found to correlate with terminal proliferation arrest in all three cell lines (HT1080, MCF7, and HCT116) in which such correlation was investigated. On the other hand, the sensitivity of the SA-β-gal assay, the background SA-β-gal levels in untreated cells, and the timing of SA-β-gal expression relative to growth arrest varied for different lines. Identification of more general and specific SLP markers should be useful for future studies on clinical tumor samples. SLP induction may also provide the basis for a screening assay for agents that would enhance terminal proliferation arrest induced by differentiating agents or low doses of cytotoxic drugs. Elucidation of the molecular determinants of senescence-like terminal proliferation arrest should suggest approaches to augmenting this desirable response and thereby increasing the efficacy of cancer treatment.

ACKNOWLEDGMENTS

We thank Dr. B. Vogelstein for HCT116 cells; Dr. F. R. Miller for MCF10AneoT cells; Drs. M. Polonskaia, K. Hagen, and J. Schnell for assistance with flow sorting; M. Chmyra and Dr. Y. Verlinsky for FISH assays; Dr. S. Salov for help with cell line maintenance; and Dr. A. V. Gudkov for helpful discussions.

REFERENCES

1. Hickman, J. A. Apoptosis induced by anticancer drugs. Cancer Metastasis Rev., *11:* 121–139, 1992.
2. Lowe, S. W., Ruley, H. E., Jacks, T., and Housman, D. E. p53-dependent apoptosis modulates the cytotoxicity of anticancer agents. Cell, *74:* 957–968, 1993.
3. Hendry, J. H., and West, C. M. L. Apoptosis and mitotic cell death: their relative contributions to normal-tissue and tumor radiation response. Int. J. Radiat. Biol., *71:* 709–719, 1997.
4. Tounekti, O., Pron, G., Belehradek, J., Jr., and Mir, L. M. Bleomycin, an apoptosis-mimetic drug that induces two types of cell death depending on the number of molecules internalized. Cancer Res., *53:* 5462–5469, 1993.
5. Lock, R. B., and Stribinskiene, L. Dual modes of death induced by etoposide in human epithelial tumor cells allow Bcl-2 to inhibit apoptosis without affecting clonogenic survival. Cancer Res., *56:* 4006–4012, 1996.
6. Torres, K., and Horwitz, S. B. Mechanisms of Taxol-induced cell death are concentration-dependent. Cancer Res., *58:* 3620–3626, 1998.
7. Demarcq, C., Bunch, R. T., Creswell, D., and Eastman, A. The role of cell cycle progression in cisplatin-induced apoptosis in Chinese hamster ovary cells. Cell Growth Differ., *5:* 983–993, 1994.
8. Merritt, A. J., Allen, T. D., Potten, C. S., and Hickman, J. A. Apoptosis in small intestinal epithelia from p53-null mice: evidence for a delayed, p53-independent G_2-M-associated cell death after γ-irradiation. Oncogene, *14:* 2759–2766, 1997.
9. Waldman, T., Lengauer, C., Kinzler, K. W., and Vogelstein, B. Uncoupling of S phase and mitosis induced by anticancer agents in cells lacking p21. Nature (Lond.), *381:* 713–716, 1996.
10. Bunz, F., Dutriaux, A., Lengauer, C., Waldman, T., Zhou, S., Brown, J. P., Sedivy, J. M. Kinzler, K. W., and Volgelstein, B. Requirement for p53 and p21 to sustain G_2 arrest after DNA damage. Science (Washington DC), *282:* 1497–1501, 1998.
11. Kung, A. L., Zetterberg, A., Sherwood, S. W., and Schimke, R. T. Cytotoxic effects of cell cycle phase specific agents: results of cell cycle perturbation. Cancer Res., *50:* 7307–7317, 1990.
12. Fornari, F. A. Jr., Jarvis, W. D., Grant, S., Orr, M. S., Randolph, J. K., White, F. K. H., Mumaw, V. R., Lovings, E. T., Freeman, R. H., and Gewirtz, D. A. Induction of differentiation and growth arrest associated with nascent (nonoligosomal) DNA fragmentation and reduced *c-myc* expression in MCF-7 human breast tumor cells after continuous exposure to a sublethal concentration of doxorubicin. Cell Growth Differ., *5:* 723–733,1994.
13. Hayflick, L., and Moorhead, P. S. The serial cultivation of human diploid cell strains. Exp. Cell Res., *37:* 585–621, 1961.
14. Smith, J. R., and Pereira-Smith, O. M. Replicative senescence: implications for *in vivo* aging and tumor suppression. Science (Washington DC), *273:* 63–67, 1996.
15. Duncan, E. L., and Reddel, R. R. Genetic changes associated with immortalization. Biochemistry, *62:* 1263–1274, 1997.
16. Dimri, G. P., Xinhua, L., Basile, G., Acosta, M., Scott, G., Roskelley, C., Medrano, E. E., Linskens, M., Rubej, I., Pereira-Smith, O., Peacocke, M., and Campisi, J. A biomarker that identifies senescent human cells in culture and in aging skin *in vivo.* Proc. Natl. Acad. Sci. USA, *92:* 9363–9367, 1995.
17. Chen, Q., and Ames, B. N. Senescence-like growth arrest induced by hydrogen peroxide in human diploid fibroblast F65 cells. Proc. Natl. Acad. Sci. USA, *91:* 4130–4134, 1994.
18. DiLeonardo, A., Linke, S. P., Clarkin, K., and Wahl, G. M. DNA damage triggers a prolonged p53-dependent G_1 arrest and long-term induction of Cip1 in normal human fibroblasts. Genes Dev., *8:* 2540–2551, 1994.
19. Robles, S. J., and Adami, G. R. Agents that cause DNA double strand breaks lead to $p16^{INK4A}$ enrichment and the premature senescence of normal fibroblasts. Oncogene, *16:* 1113–1123, 1998.
20. Serrano, M., Lin, A. W., McCurrach, M. E., Beach, D., and Lowe, S. W. Oncogenic ras provokes premature cell senescence associated with accumulation of p53 and p16INK4a. Cell, *88:* 593–602, 1997.
21. Weinberg, R. A. The cat and mouse games that genes, viruses and cells play. Cell, *88:* 573–575, 1997.
22. Ko, L. J., and Prives, C. p53: puzzle and paradigm. Genes Dev., *10:* 1054–1072, 1996.
23. Linke, S. P., Clarkin, K. C., and Wahl, G. M. p53 mediates permanent arrest over multiple cell cycles in response to γ-irradiation. Cancer Res., *57:* 1171–1179, 1997.
24. Whitaker, N. J., Bryan, T. M., Bonnefin, P., Chang, A. C-M., Musgrove, E. A., Breithwaite, A. W., and Reddel, R. R. Involvement of RB-1, p53, $p16^{INK4}$ and telomerase in immortalization of human cells. Oncogene, *11:* 971–976, 1995.
25. Shay, J. W. Telomerase in human development and cancer. J. Cell Physiol., *173:* 266–270, 1997.
26. Pereira-Smith, O. M., and Smith, J. R. Genetic analysis of indefinite division in human cells: identification of four complementation groups. Proc. Natl. Acad. Sci. USA, *85:* 6042–6046, 1988.
27. Sugrue, M. M., Shin, D. Y., Lee, S. W., and Aaronson, S. A. Wild-type p53 triggers a rapid senescence program in human tumor cells lacking functional p53. Proc. Natl. Acad. Sci. USA, *94:* 9648–9653, 1997.
28. Xu, H-J., Zhou, Y., Ji, W., Perng, G-S., Kruzelock, R., Kong, C-T., Bast, R. C., Mills, G. B., Li, J., and Hu, S-X. Reexpression of the retinoblastoma protein in tumor cells induces senescence and telomerase inhibition. Oncogene, *15:* 2589–2596, 1997.
29. Uhrbom, L., Nister, M., and Westermark, B. Induction of senescence in human malignant glioma cells by $p16^{INK4A}$. Oncogene, *15:* 505–514, 1997.
30. Vogt, M., Haggblom, C., Yeargin, J., Christiansen-Weber, T., and Haas, M. Independent induction of senescence by $p16^{INK4a}$ and $p21^{CIP1}$ in spontaneously immortalized human fibroblasts. Cell Growth Differ., *9:* 139–146, 1998.
31. Wang, X., Wong, S. C., Pan, J., Tsao, S. W., Fung, K. H., Kwong, D. L., Sham, J. S., Nicholls, J. M. Evidence of cisplatin-induced senescent-like growth arrest in nasopharyngeal carcinoma cells. Cancer Res., *58:* 5019–5022, 1998.
32. Chang, B-D., and Roninson, I. B. Inducible retroviral vectors regulated by *lac* repressor in mammalian cells. Gene, *183:* 137–142, 1996.
33. Perry, M. E., Rolfe, M., McIntyre, P., Commane, M., and Stark, G. R. Induction of gene amplification by 5-aza-2′-deoxycytidine. Mutat. Res., *276:* 189–197, 1992.
34. Jordan, M. A., Wendell, K., Gardiner, S., Derry, W. B., Copp, H., and Wilson, L. Mitotic block induced in HeLa cells by low concentrations of paclitaxel (Taxol) results in abnormal mitotic exit and apoptotic cell death. Cancer Res., *56:* 816–825, 1996.
35. Brown, R., Marshall, C. J., Pennie, S. G., and Hall, A. Mechanism of activation of an N-*ras* gene in the human fibrosarcoma cell line HT1080. EMBO J., *3:* 1321–1326, 1984.
36. Li, W., Fan, J., Hochhauser, D., Banerjee, D., Zielinski, Z., Almasan, A., Yin, Y., Kelly, R., Wahl, G. M., and Bertino, J. R. Lack of functional retinoblastoma protein mediates increased resistance to antimetabolites in human sarcoma cell lines. Proc. Natl. Acad. Sci. USA, *24:* 10436–10440, 1995.
37. Pellegata, N. S., Antoniono, R. J., Redpath, J. L., and Stanbridge, E. J. DNA damage and p53-mediated cell cycle arrest: a reevaluation. Proc. Natl. Acad. Sci. USA, *93:* 15209–15214, 1996.
38. Horan, P. K., and Slezak, S. E. Stable cell membrane labeling. Nature (Lond.), *340:* 167–168, 1989.
39. Sherwood, S. W., Rush, D., Ellsworth, J. L., and Schimke, R. T. Defining cellular senescence in IMR-90 cells: a flow cytometric analysis. Proc. Natl. Acad. Sci. USA, *85:* 9086–9090, 1988.
40. Ueda, H., Takenawa, T., Millan, J. C., Gesell, M. S., and Brandes, D. The effects of retinoids on proliferative capacities and macromolecular synthesis in human breast cancer MCF-7 cells. Cancer (Phila.), *15:* 2203–2209, 1980.
41. Guilbaud, N. F., Gas, N., Dupont, M. A., and Valette, A. Effects of differentiation-inducing agents on maturation of human MCF-7 breast cancer cells. J. Cell Physiol., *145:* 162–172, 1990.
42. Miller, F. R., Soule, H. D., Tait, L., Pauley, R. J., Wolman, S. R., Dawson, P. J., and Heppner, G. H. Xenograft model of progressive human proliferative breast disease. J. Natl. Cancer Inst., *85:* 1725–1732, 1993.
43. Moon, R. C., Mehta, R. G., and Rao, K. V. N. Retinoids and cancer in experimental animals. *In:* M. B. Sporn, A. B. Roberts, and D. S. Goodman (eds.), The Retinoids, Biology, Chemistry, and Medicine, pp. 573–595. New York: Raven Press, 1994.
44. Holt, S. E., Aisner, D. L., Shay, J. W., and Wright, W. E. Lack of cell cycle regulation of telomerase activity in human cells. Proc. Natl. Acad. Sci. USA, *94:* 10687–10692, 1997.
45. Vaziri, H., West, M. D., Allsopp, R. C., Davison, T. S., Wu, Y. S., Arrowsmith, C. H., Poirier, G. G., and Benchimol, S. ATM-dependent telomere loss in aging human diploid fibroblasts and DNA damage lead to the post-translational activation of p53 protein involving poly(ADP-ribose) polymerase. EMBO J., *16:* 6018–6033, 1997.
46. Chang, B. D., Xuan, Y., Broude, E. V., Zhu, H., Schott, B., Fang, J., and Roninson, I. B. Role of p53 and $p21^{waf1/cip1}$ in senescence-like terminal proliferation arrest induced in human tumor cells by chemotherapeutic drugs. Oncogene, 1999, in press.
47. Speth, P. A., Linssen, P. C., Boezeman, J. B., Wessels, H. M., and Haanen, C. Cellular and plasma adriamycin concentrations in long-term infusion therapy of leukemia patients. Cancer Chemother. Pharmacol., *20:* 305–310, 1987.
48. Debernardis, D., Sire, E. G., DeFeudis, P., Vikhanskaya, F., Valenti, M., Russo, P., Parodi, S., D'Incalci, M., and Broggini, M. p53 status does not affect sensitivity of human ovarian cancer cell lines to paclitaxel. Cancer Res., *57:* 870–874, 1997.
49. Diller, L., Kassel, J., Nelson, C. E., Gryka, M. A., Litwak, G., Gebbardt, M., Bressac, B. Ozturk, M., Baker, S. J., Vogelstein, B., and Friend, S. H. p53 functions as a cell cycle control protein in osteosarcomas. Mol. Cell. Biol., *10:* 5772–5781, 1990.
50. Hosono, S., Lee, C. S., Chou, M. J., Yang, C. S., and Shih, C. H. Molecular analysis of the *p53* alleles in primary hepatocellular carcinomas and cell lines. Oncogene, *6:* 237–243 1991.
51. Kim, M. S., Li, S. L., Bertolami, C. N., Cherrick, H. M., and Park, N. H. State of p53, Rb and DCC tumor suppressor genes in human oral cancer cell lines. Anticancer Res., *13:* 1405–1413, 1993.
52. O'Connor, P. M., Jackman, J., Bae, I., Myers, T. G., Fan, S. Mutoh, M., Scudiero, D. A., Monks, A., Sausville, E. A., Weinstein, J. N., Friend, S., Fornace, A. J., Jr., and Kohn, K. W. Characterization of the p53 tumor suppressor pathway in cell lines of the National Cancer Institute anticancer drug screen and correlations with the growth-inhibitory potency of 123 anticancer agents. Cancer Res., *57:* 4285–4300, 1997.
53. Rodrigues, N. R., Rowan, A., Smith, M. E. F., Kerr, I. B., Bodmer, W. F., Gannon, J. V., and Lane, D. P. p53 mutations in colorectal cancer. Proc. Natl. Acad. Sci. USA, *87:* 7555–7559, 1990.
54. Scheffner, M., Munger, K., Byrne, J. C., and Howley, P. M. The state of p53 and retinoblastoma genes in human cervical carcinoma cell line. Proc. Natl. Acad. Sci. USA, *88:* 5523–5527, 1991.
55. Yaginuma, Y., and Westphal, H. Analysis of the *p53* gene in human uterine carcinoma cell lines. Cancer Res., *51:* 6506–6509, 1991.

EFFICIENT RECOVERY AND REGENERATION OF INTEGRATED RETROVIRUSES.

B. Schott, E. S. Kandel, I. B. Roninson.
University of Illinois at Chicago, Department of Genetics.

We developed a rapid and efficient PCR-based rescue procedure for integrated recombinant retroviruses. Genomic DNA of infected cells is subjected to Long and Accurate PCR (LA PCR) with a pair of primers derived from the long terminal repeats (LTRs), and infectious viral particles are generated by transfecting appropriate packaging cells with the purified LA PCR product. Sensitivity of LA PCR allows us to regenerate functional retroviruses from nanogram quantities of genomic DNA. Similar yields of infectious virus were obtained upon transfecting Bosc23 packaging cells with either LA PCR amplified provirus or with the same construct within a supercoiled plasmid, suggesting that expression of LTR promoter is similar in both cases. The new procedure accurately maintains representation of individual variants in mixed populations of proviruses and has been successfully used in our laboratory to transfer retroviral libraries for subsequent rounds of expression selection. As compared to the currently used protocols, the new procedure offers substantial savings of time and labor: functional retrovirus can be regenerated from infected cells in as little as three to four days. We suggest that, besides recovery and regeneration of retroviral vectors, this procedure may be useful for the analysis of natural populations of retroviruses, including HIV.

Cold Spring Harbor Laboratory Meeting "Retroviruses"
Cold Spring Harbor, NY (1997)

NOVEL RETROVIRAL VECTORS EXPRESSING RED-SHIFTED VARIANTS OF GREEN FLUORESCENT PROTEIN.

E. S. Kandel, B. Schott, B.-D. Chang, A. V. Gudkov, I. B. Roninson.
University of Illinois at Chicago, Department of Genetics.

We developed an extensive series of retroviral vectors that utilize the gene for green fluorescent protein (GFP) as a marker. We have used "red-shifted" S65T mutant and its improved derivatives (*Green Lantern* from Life Technologies and *EGFP* from Clontech) that can be detected using common fluorescent microscopes or flowcytometers. Our constructs were derived from pLNCX and pBabe vectors and vary in the arrangement of promoters and cloning sites. To expand the range of possible applications we used *EGFP* in a construct with an LTR optimized for expression in embryonic stem cells. We have also substituted *neo* marker in IPTG-regulated retroviral vectors (Chang at al., Gene 183, 137-142, 1996) for *Green Lantern.*

Our vectors were successfully tested in transduction and transfection experiments on a broad variety of cells representing different tissues of human, rat and murine origin, including murine bone marrow cells. FACS analysis of infected cells revealed an appearance of a transduced population that was, depending on the particular vector-host combination, 5 to 700 times brighter than the parental cells. Positive fluorescence was detectable by flowcytometry the next day after infection and reached its maximum one to two days later. Transduced cells can be reliably selected by FACS without loss of viability, and the sorted population remains close to 100% positive after prolonged cultivation. By selecting only the brightest infectants we were able to obtain populations with higher than average number of integrated proviruses.

GFP expressed from our vectors has no cytotoxic or cytostatic effect. Also, GFP expression does not interfere with tumorigenicity of HT1080 in nude mice and bright green fluorescence is readily detectable in tumor samples. Since vectors with different forms of GFP or different promoter combinations render different intensity of fluorescence, it is possible to select pairs of constructs that produce two distinct positive populations of infectants identifiable by FACS. This allows us to monitor gene delivery into cells that already express certain amount of GFP or to tag and track one or two subpopulations in a complex cell mixture.

Cold Spring Harbor Laboratory Meeting "Retroviruses"
Cold Spring Harbor, NY (1997)

GFP IN RETROVIRAL VECTORS: APPLICATIONS AND LESSONS.

E.Kandel, B.Chang, B.Schott, A.Shtil, V.Levenson, A.Gudkov, I.Roninson. Dept. of Molecular Genetics, Univ. of Illinois at Chicago, Chicago, IL, 60607.

The common selectable markers for retroviral transduction (such as *neo*) require lengthy and artifact-prone drug selection of infected cells. We have studied the applicability of GFP as a marker gene in retroviral vectors by analyzing the expression of GFP and a cotransduced gene in various vector designs. Wild type GFP did not provide adequate fluorescence, while the expression of "red-shifted" GFPS65T was detectable in some but not all constructs. By testing different promoter combinations and "humanized" GFP variants, we obtained vectors for optimal expression of the cotransduced gene and reliable detection of GFP fluorescence. Cells harboring such constructs are detectable by fluorescence microscopy, multi-well fluorescence reading and flow cytometry; GFP fluorescence is also detectable in tumors growing *in vivo*. GFP expression has no detrimental effects on the infectants and does not alter the tumorigenicity of transformed cells. The use of GFP permits several specific applications. (a) Selection of the brightest infectants enriches for multiply infected cells. (b) In retroviral vectors containing an inducible promoter transcribed in the opposite orientation to GFP, antisense inhibition of GFP expression provides a marker for promoter induction. (c) Using two vectors that confer markedly different levels of fluorescence, one can simultaneously monitor two transduced cell populations by flow cytometry. We can also distinguish transduced populations harboring "red-shifted" and "blue" GFPs. (d) Long-term dynamics of GFP-positive fractions in a mixed population can be used to monitor the biological effects of a cotransduced gene. Overall, the use of GFP in retroviral vectors has extended the range of applications for retroviral transduction and provided valuable insights for the design of retroviral vectors.

International Symposium on Green Fluorescent Protein

New Brunswick, NJ (1997)

metabolism enzymes, and it is believed to act via a novel mechanism. Studies aimed at elucidating the mechanism of action of CB30865 have focused on characterization of a resistant cell line (W1L2:R865), raised from the W1L2 human lymphoblastoid line, with ~200 fold acquired resistance to CB30865 (W1L2 IC_{50} ~3 nM; W1L2:R865 IC_{50} ~600 nM). Comparative genomic hybridization (CGH) was used to identify areas of genetic amplification or deletion in the resistant line which may be related to the mechanism of action of CB30865. DNA was extracted from W1L2 and W1L2:R865 lines, labelled with digoxigenin or biotin respectively, hybridized onto normal metaphase chromosomes and detected by immunofluorescence. A high-level amplification on the long arm of chromosome 7 (region q22) was observed. Fluorescence *in situ* hybridization (FISH) was performed with a panel of YAC clones spanning region 7q22, by hybridization to metaphase chromosomes isolated from the sensitive and resistant pair of cell lines. This allowed the area of peak amplification to be isolated to one YAC (~1.5 MB). Current studies are aimed at identifying the gene(s) involved in the amplicon and relating this to the target of CB30865. *Sponsored by the Cancer Research Campaign.*

#2818 A combination of genetic suppressor elements produces resistance to drugs inhibiting DNA replication. Levenson V.V., Lausch E., Libants S., Kirschling D.J., Kandel E., Roninson I.B. *Department of Molecular Genetics, University of Illinois at Chicago, Chicago, IL, 60607.*

Many anticancer drugs inhibit DNA replication. To understand the role that the inhibition of replication plays in drug-induced cell death, we have investigated the molecular determinants of the sensitivity of human HT1080 fibrosarcoma cells to DNA replication inhibitor aphidicolin (Aph). To identify genes that potentiate the Aph cytotoxicity, we have carried out the selection of genetic suppressor elements (GSEs; short cDNA fragments coding for inhibitory antisense RNA or dominant negative peptides) that would confer resistance to Aph. A retroviral expression library, carrying short fragments of normalized cDNA from HeLa cells, was used to carry out three consecutive rounds of transduction, Aph selection, and recovery of retroviral inserts from the surviving cells. The sublibrary, isolated after this selection, conferred resistance to Aph. All the resistant cell lines isolated after infection with this sublibrary carried multiple cDNA inserts. A combination of the most abundant clones provided resistance to Aph. Omission of any clone from this set greatly decreased this effect, suggesting that the four GSEs act in combination. Transduced cell lines carrying all four GSEs show cross-resistance to Aph, mimosine, cytarabine and doxorubicin The nature of these genes and their mechanism of action are currently under investigation.

#2819 The influence of mitochondrial activity on doxorubicin sensitivity and induced apoptosis in human squamous carcinoma A431 cells. Timothy W.L. Wong, L.Y. Chung, H.Y. Yu, and T.T. Kwok. *Department of Biochemistry, The Chinese University of Hong Kong, Hong Kong.*

Doxorubicin (DOX) resistant A10A cells were derived from human squamous carcinoma A431 cells. In addition to difference in drug sensitivity, DOX induced a greater extent of apoptosis in parent cells than in A10A cells as demonstrated by DNA fragmentation assay. Results from Western blot analysis indicated that the expressions of P-glycoprotein, glutathione-S-transferase, and topoisomerase II were similar between the two cell lines. To investigate the underlying mechanisms for DOX resistance in A431 cells, RT-PCR based differential display was used to identify genes which are differentially expressed in the drug resistant cells. Among the clones identified, two were found to have sequence homology with the mitochondrial encoded NADH dehydrogenase subunit III and cytochrome c oxidase subunit II. Using Northern blot analysis, the expression of these two mitochondrial genes were down-regulated in the drug resistant cells as compared to the parent cells. Results from the preliminary study suggested that mitochondrial activity may regulate drug sensitivity and apoptosis in cells. To further understand the relationship, experiments examining the expression and the activities of the enzymes in mitochondrial electron transport chain of A431 cells are currently underway and the results will be presented.

#2820 Reversal of acquired drug resistance in murine lymphoma cells ...ing transfection of a novel gene. Shen, S., and Hwang, P.L. *Department ...ology, National University of Singapore, Republic of Singapore 119260.*

... studying the cytotoxic effects of oxygenated derivatives of cholesterol ...), we cultured the murine lymphoma cell line EL4 in the presence of ... concentrations of an oxysterol (7-ketocholestanol), and derived a ... cell line, EL4R, which exhibited resistance not only against the cytotoxic ... oxysterols, but also against that of a number of anti-cancer drugs ... vincristine, etoposide, cisplatin, and tamoxifen. The resistance of the ... to these cytotoxic compounds remained stable for at least 14 weeks ...cholestanol ...

vector alone ($p < 0.01$ in all cases). These studies sugg did not match DNA sequences in available database gene whose expression confers increased susceptibili toxic drugs.

#2821 Novel mechanisms of 1,3-bis(2-chloroeti tance in human malignant gliomas. Scheck, A.C., Rh Rojanala, S., Furlong, R.J. and Steinway, M.L. *Neuro-Oı Neurological Institute, Phoenix, AZ 85013.*

Alkylating agents such as 1,3-bis(2-chloroethyl)-1-nit tinely used in the treatment of human malignant glioma these tumors typically recur, leading to patient morta tumor obtained from patients treated with BCNU are (cells from the primary tumor. These resistant cells are t the over-representation of part or all of chromosomes *situ* hybridization is being used to identify the region o retained in BCNU resistant cells, and differential mRNA identify genes involved in such resistance. Our experim altered expression of p53-induced gene 8 (PIG8) may tumors when compared to primary tumors from the sam from recurrent tumors do not always have more p53 r primary tumors, and the role of this gene in BCNU resi investigation. The retinoic acid-induced gene 14-1 (RI(differentially expressed in these tumor cells; however unknown, and its role in the survival of these cells is nc

#2822 Role of *E2F-4* mutations in chemosensitiv K., Takashima, H., Kawashima, T., Tanaka, N., Shimizu *Medical School, 2-5-1 Shikata-cho, Okayama 700-8558*

We have recently identified the tumor specific mutatic satellite (AGC) repeats, encoding 13 serine residues, region in sporadic colorectal cancer with microsatellite ir HNPCC. The effect of the mutations of the *E2F-4* on commonly used chemotherapeutic agents were tested transfected with expression vectors carrying wild type *E2F-4*. *E2F-4* overexpression selectively sensitize the ce inhibitor etoposid. However, *E2F-4* mutants including in repeat locus were associated with less sensitive to etop the *E2F-4* mutants was sensitive to carboplatin (CBDC showed resistance to the agent. Only the mutant tran addition to the repeat unit of the *E2F-4* showed resistant t other mutant as well as wild type *E2F-4* cell lines. Other c including 5-FU, CDDP, adriamycin caused no altered transfected with wild type as well as mutant *E2F-4*.

#2823 Induction of E2F-1 in response to drug-ind the human HT-29 colon carcinoma cell line. Pilon, A.A. Pommier. *Laboratory of Molecular Pharmacology, Divis National Cancer Institute, NIH, Bethesda, MD, 20892.*

The E2F family of transcription factors regulates the tra phase of the cell cycle. Overexpression of E2F-1 not or phase but can also induce apoptosis. We have examined in HT29 following exposure to different anticancer agent induces apoptosis in this cell line. Treatment with campto gamma irradiation or taxol increased E2F-1 protein level to an increase in E2F-1 protein levels as early as 3 ho peaked at 24 hours, well before the onset of DNA fra cleavage. This rapid induction of E2F-1 was correlated cyclin B1 and the accumulation of cells in G2/M phase results suggest that E2F-1 is a stress-inducible factor cellular response to various anticancer agents, possibly t lating cell cycle progression and apoptosis.

#2824 Critical role of cyclooxygenase-2 in sens cancer cells to anticancer agents. Hiroshi Nokihar Tsutomu Shinohara, Hiroaki Yanagawa and Saburo Sone *of Internal Medicine, The University of Tokushima School c cho 3, Tokushima, Japan.*

Drug resistance is a critical problem in the chemoth cancer. In this study, we examined the role of cyclaox sensitivity to anticancer drugs in lung cancer cells. For t

ɔprèssion of spermidine/spermine N[1]-
jrowth and enhances sensitivity to the
ıor𝐬permine (DENSPM). Vujcic, S.,
ɔswell Park Cancer Institute, Buffalo, NY,
ity of Kuopio, Kuopio Finland.
ntly undergoing Phase II clinical evalua-
amine biosynthesis, the analog potently
me SSAT. To further address the role of
amine pools and cell growth, we have
arcinoma cells containing a SSAT gene
ble system. Removal of doxycycline for
RNA and a 10-fold increase in enzyme
nine pools were depleted by ~50–75%
mine pools increased significantly. Cell
cells grown in presence of doxycycline
is sufficient to reduce cell growth rate.
with 10 μM DENSPM caused a much
lls, which were not overexpressing the
n of SSAT is an important determinant
eutic strategies, which increase SSAT
rapy. (Supported by CA-76429).

lase responsible for phenylbutyrate
on in myeloid neoplasms? Fu, S. and
Center, Baltimore, MD 21287-8963.
minal differentiation, and apoptosis in
ited clinical activity in Phase I trials in
f PB appear more similar to sodium
ent among the numerous molecular
e deacetylase, similar to SB. We have
cs of PB for changes in histone acet-
nd examined the pharmacodynamic
or Trichostatin A (TSA) in the ML-1
e cultured in the presence or absence
aluation of differentiation, cell cycle
21$^{WAF1/CIP1}$. Unlike PB, TSA did not
ed to rapid induction of expression of
se of TSA in contrast to PB treatment
was a strong inducer of apoptosis
optosis induction by PB is twice that
t. Incubation of ML-1 cells with PB
doses ranging from 1 to 5 mM; all
nduced within this dose range. While
cetylation in ML-1 cells, these data
e in myeloid leukemia cells may not
ions of PB.

abolism block migration of human
Berens M.E.* Dept. Neurosurgery,
urg, Germany *Dept. Neuro-Oncol-
Arizona, USA.
fied thromboxane synthase (Thxsyn)
a cells. We have characterized the
ll as Thxsyn in glioma cell lines and
ibitors of these enzymes were used
ro. RT-PCR demonstrated Thxsyn
astrocytes did not express Thxsyn.
and 10 of 11 cell lines respectively,
evels. Immunohistochemistry dem-
liomas of various grads with high
ed and focal expression in the most
ated the highest proliferation rates.
mboxane-B2 expression by ELISA.
ihibitors of Thxsyn and COX were
indomethacin and imidazole had
ihibitors furegrelate and dazmegrel
t manner to levels of non-specific
as slightly enhanced in a substrate

... 1998, 4, 3078–3086). The delayed functional cardiotoxic effects (ECG analysis, haemodynamics and isoprenaline-induced cardiac responses) of treatment with equimyelotoxic regimen of MEN 10755 and doxorubicin (1.5 mg/kg i.v. weekly for five times) were investigated (at 4 and 13 weeks after the last treatment) in anaesthetized rats. Doxorubicin induced significant ECG alterations (prolongation of QαT and SαT intervals) starting from 2 days after last treatment. These cardiotoxic effects were progressive being further worsened after 4 and 13 weeks of recovery period. MEN 10755 induced ECG alterations similar in nature but of lesser severity compared to doxorubicin and in addtion with no progression at 13 as compared to 4 weeks. Significative reduction in mean arterial pressure, heart rate and adrenergic stimulation of contractile performance (LVSP and dP/dt) was also observed, at week 4 and 13, in animals receiving doxorubicin but not MEN10755. In conclusion, with an equimyelotoxic regimen, MEN 10755 produced, as compared to doxorubicin, a minor ECG alterations and cardiac performance impairment. In addition a progressive delayed deterioration (at 13 weeks) of cardiac toxicities was evident in doxorubicin- but not in MEN 10755-treated rats.

#87 Potentiation of doxorubicin (DOX)-induced apoptosis by N-benzyladriamycin-14-valerate (AD198). Koseki Y, Roaten JB, Savranskaya L, Lothstein L, Rodrigues PJ, Israel M, and Sweatman TW. *University of Tennessee College of Medicine, Memphis, TN 38163.*

AD 198, a novel lipophilic anthracycline, is capable of circumventing multiple forms of DOX resistance (P-gp, MRP and Bcl-2 overexpression; at-MDR). Recent studies have shown that AD 198 is a potent PKC inhibitor while its principal metabolite, N-benzyladriamycin (AD 288) and DOX are virtually devoid of this activity. In light of these findings, we have re-examined our previous observation that low doses of AD 198 potentiate the cytotoxicity of DOX (clonogenic assay) in human ovarian (OVCAR-3) carcinoma cells (Koseki et al Proc. AACR 37: 334, 1996). The effects of AD 198 and AD 288 on DOX-induced apoptosis (bisbenzamide staining) in these cells were determined using conditions [DOX (4.0 μm) $\pm$ AD 198 or AD 288 (0.3 μm): 3-hr exposure] identical to those used earlier. At 48-hr and 72-hr following drug exposure, apoptotic indices were control (1.7% *vs.* 1.9%), DOX alone (2.7% *vs.* 3.5%), AD198 alone (1.7% *vs.* 3.2%) and DOX+AD198 (8.5% *vs.* 11.2%). By contrast, AD 288 (2.9% and 3.2% apoptotic cells at 48-hr and 72-hr, resp.) was without additional effect when admixed with DOX. Thus, the previously reported synergistic effects of AD 198 appear to correlate with the PKC-modulatory activity of this novel compound.

#88 Low doses of anticancer agents induce a senescence-like phenotype and mitotic death in human tumor cells. Chang, B.-D., Broude, E.V., Zhu, H., Xuan, Y., Dokmanovic, M., Ruth, A., Kandel, E.S., Lausch, E., Christov, K., and Roninson, I.B. *Depts. of Molecular Genetics and Surgical Oncology (K.C.), University of Illinois at Chicago, Chicago, IL 60607.*

Exposure of human HT1080 fibrosarcoma cells to moderate doses of different anticancer drugs and ionizing radiation induces two major non-exclusive responses in the treated cells. The first response, induced in 45–66% of the cells after 4 day exposure to ID_{85} doses of all the tested agents, is mitotic death characterized by the formation of multiple micronuclei. The second response, induced by most agents in 15–79% of the cells, was the appearance of cells that express senescence-associated β-galactosidase (SA-β-gal) and morphologic features of senescent fibroblasts. SA-β-gal+ cells that survive doxorubicin treatment show increased DNA ploidy and proliferative changes associated with senescence, including decreased DNA replication, growth arrest after a small number of cell divisions, and loss of long-term clonogenic potential. Doxorubicin treatment induced features of senescence in 10 of 13 tested cell lines derived from different types of human solid tumors, including all the tested lines with wild-type p53 and half of p53-mutated lines. SA-β-gal expression was also observed in a breast cancer xenograft model after *in vivo* retinoid treatment. Induction of tumor cell senescence may provide an important component of treatment response in clinical cancer.

#89 Activation of MAP kinase during apoptosis mediated by vinorelbine in MCF-7 cells. Wang, LG., Liu, XM., Kreis, W., Budman, DR., Adams, LM. *Don Monti Division of Med. Oncol., NYU School of Medicine, North Shore University Hosp., Manhasset, New York 11030, and Glaxo Wellcome Inc., 5 Moore Drive, Research Triangle Park, NC, 27709.*

Vinorelbine (Navelbine) is a third-generation vinca alkaloid frequently used alone or in combination with other anticancer drugs. Our recent study established